Development of a hybrid wheat straw adsorption and microfiltration system for oily wastewater treatment

by

Kavya Suresh

A thesis submitted in partial fulfillment of the requirements for the degree of

Master of Science

Department of Mechanical Engineering

University of Alberta

Abstract

Effective, economical, and sustainable treatment technologies are highly desirable for treating oily wastewater generated from various industries as well as municipal and commercial establishments. The performance of traditional polymeric membranes is largely constrained by their high fouling tendency to oil and hence renders this highly efficient technology for separating emulsified oil inappropriate. Therefore, a unique integrated treatment train coupling polyamide-imide (PAI) microfiltration membrane with an adsorption system using a chemically modified agricultural by-product, wheat straw, was implemented to decrease the fouling and increase the membrane life span. In the first work, we modified wheat straw through a simple radical polymerization to graft biocompatible PMMA in order to enhance the hydrophobicity. The substantial increase in oil adhesivity after grafting PMMA was evident from the 0° oil contact angle for PMMA-g-WS film. Oil absorptivity was thoroughly evaluated by batch oil adsorption study using variable adsorbent dosages and oil emulsion concentrations. The PMMA-g-WS exhibited the highest oil adsorption capacity of *ca.* 1129 mg/g, as determined by the kinetic equilibrium study. The adsorption capacity was explicitly high compared to that of the pristine (*ca.* 346 mg/g) and pre-treated (*ca.* 741 mg/g) samples due to exposure of numerous mesopores and micropores and which made an avenue for deeper oil penetration. The shape of the hysteresis loops indicated the predominance of mesopores in all three samples, which was also confirmed by the pore width values ranging from 1.6-32 nm. In addition, the strong hydrophobic interactions due to the grafted surface functionalities significantly added to the oil adsorptivity. Langmuir and Freundlich adsorption isotherms were applied to evaluate the adsorption mechanism. The experimental data fitted well with Freundlich isotherm, indicating a multilayer adsorption process and heterogeneity of adsorption sites.

On the other hand, they also fitted well with the pseudo-second-order rate equation with R^2 as high as 0.999. This also indicated indicate multilayer adsorption where the initial rate of monolayer adsorption is faster than the rate of subsequent multilayer formation. The high oil adsorption capacity of the PMMA-g-WS makes it a very promising material oily wastewater treatment. This will simultaneously resolve issues with the treatment of oily wastewater and the handling of abundant quantities of waste wheat straw.

In the second work, the breakthrough curves for different oil concentrations were obtained using a bench-scale set up of a fixed-bed column. The oil removal efficiency decreased only by 18% during the subsequent cycle after regeneration for 100 ppm oil concentration. This system was then coupled with the PAI membrane fabricated by the non-solvent induced phase separation technique. Polyvinylpyrrolidone (PVP) was blended to enhance the hydrophilicity. The flux decline was as low as 4% for 100 ppm feed with pre-treatment and 40% for the feed without pre-treatment. More importantly, the pre-treatment increased the FRR from 84% to 95% in the case of 200, 300, and 500 ppm feed. The performance of commercial PES membranes was compared with the fabricated PAI. They exhibited a higher flux recovery ratio (FRR) for the pre-treated feed in case of low oil concentrations. Higher oil concentrations, however, caused irreversible fouling of the membrane by pore blocking, as a result of which the FRR was very poor after regeneration. Therefore, the results indicated an exceptional improvement in flux and FRR for pre-treated oil emulsions. Also, the PAI membranes exhibited robust performance during the consecutive two cycles; each provided 100% removal efficiency for oil. The integration of adsorption with naturally derived eco-friendly and cost-effective wheat straw grafted with PMMA and PAI microfiltration system offered outstanding oil removal and prolonged the membrane lifespan at the same time as the membrane fouling was diminished.

Preface

This thesis is an original work by Kavya Suresh. No part of this thesis has been previously published. highlights the first applications of integrated poly(methyl methacrylate) grafted wheat straw and polyamide-imide microfiltration membrane for separation of oil and water.

Chapter 2 of the thesis, “Enabling the agricultural waste wheat straw for the economical and eco-friendly treatment of oily wastewater by simple modification with poly(methyl methacrylate)” , has been prepared for submission.

Chapter 3 of the thesis, “Integration of poly(methyl methacrylate) grafted adsorption and polyamide-imide microfiltration membranes for separation of oil and water”, is also being prepared for submission.

Acknowledgement

I express my profound gratitude to my supervisor Dr. Mohtada Sadrzadeh for his guidance and encouragement throughout this program. I'm grateful to him for giving me this wonderful opportunity and being extremely supportive and patient during my tough times. I also like to extend my gratitude co-supervisor to Dr. Brian Fleck for his support and guidance. The discussions I had with him really helped me to cope with challenging times.

I would like to thank my teammate Muhammad Amirul Islam, for his valuable guidance and insights, and I also want to extend my thanks to Masoud Rastgar for his support and guidance. I thank my teammates Asad Asad, Pooria Karami, and Sadegh Aghapour, for their immense support and belief in me. The discussions and insights they provided me helped immensely in my research. I also thank Amirreza Sohrabi, Nandini Debnath, Nusrat Helali, and Farhad Ismail for their valuable suggestions. I also thank my husband, Ajay Ganesh, for his immense support and encouragement.

I dedicate this thesis to my father, because of who I'm here today. His support can't be described in words. I thank him for being with me always as a guide, companion, and my best friend. I also want to thank my mother for her immense love and support.

Table of Contents

List of figures

List of tables

Chapter 1: Introduction

1.1 Background and Overview

In the present era, the pollution of water bodies due to the influx of wastewater from industries and other point sources has become a serious issue globally. Oil is one of the significant pollutants resulting in the deterioration of water quality and has raised public concern. The broad list of oily wastewater generating sources includes oil industries, oil refineries, petrochemical industries, food industry, dairy industry, and municipal wastewaters [1,2]. Oily wastewaters carry several toxic and carcinogenic compounds such as benzene, polycyclic aromatic hydrocarbons (PAHs), and hydrofluoric acid. One of the serious implications of discharge of these lethal compounds includes ecological hypoxia (oxygen depletion) in water bodies since oil floats on water due to low specific gravity. This phenomenon leads to the death of aquatic plants and animals. Apart from that, it also deteriorates the groundwater quality as well as air quality as a result of the evaporation of volatile compounds into the atmosphere [3]. For countries such as Canada, which holds the world's third-largest oil reserves and produces approximately 1.2 million barrels of conventional oil per day, the need for developing efficient technologies for managing oily wastewater streams is vital. Some of the stringent standards, including the Canadian regulations for discharge of oil into the sea, requiring the hydrocarbon content to be less than 5ppm in discharge water, also calls for efficient separation of oil and water from effluents [4].

Most of the industries generate stabilized emulsions that fail to form distinctive layers of oil and water, thus making separation by gravity settling impossible. Numerous other conventional methods such as coagulation and flocculation [5], adsorption using granular activated carbon [6], dissolved air flotation [7], activated sludge process [8] have been applied to separate oil and water. However, these techniques have limited effectiveness in separating the emulsified oil content with a droplet size of $\leq$20 μm [9]. Membrane filtration with pore sizes ranging from micrometer to nanometer has been acknowledged as a highly efficient technique for separating emulsified oil [9,10]. High removal efficiency, small footprint, minimal chemical requirement, and the ability to maintain consistent effluent quality are some of the major benefits of the membrane filtration process [11]. However, the biggest challenge is the extensive fouling of the widely used polymer

membranes as a result of their intrinsic oleophilic property. This results in cake formation due to the adhesion of oil on the surface or pore plugging [12]. Even though hydrophilicity can be improved by surface modification, blending, and grafting, the performance remains limited.

In order to overcome the flux decline by fouling and to augment the membrane lifespan, an ideal way is to pre-treat the oil containing effluent using a simple technique. Numerous works reported the improvement in performance in terms of flux and rejection and, more importantly, the membrane lifespan by having a pre-treatment before membrane filtration [7,13,14]. Integration of activated carbon and bentonite adsorption system with PES nano-silica membranes were found to increase the flux significantly by 26.4-30.6% along with providing high rejection of 72% and 90% for TDS and salinity, respectively [15]. In another work [16], precipitative softening and walnut shell filtration as pre-treatment for membrane distillation displayed exceptional efficiencies (≥95%) in eliminating volatile and toxic components such as BTEX (benzene, toluene, ethylbenzene, xylene) from produced water.

The adsorption process is found to be promising as it is a simple, sustainable, and efficient technique to be used as a preliminary treatment system for membrane filtration. The most common traditional adsorbent used for oil-water separation is activated carbon. Activated carbon systems, however, are not economical and require rigorous regeneration of spent carbon due to its highly porous structure [17–19].

Recent interfacial studies related to adsorption are mainly focused on utilizing natural organic materials such as agricultural by-products as an alternative to traditional adsorbents. Agricultural wastes used as adsorbents for treating hydrocarbon-containing effluents include corn straw fibers [20], rice husk [21,22], cotton fiber [23], and banana peels [24] to name a few. These agricultural by-products are lignocellulosic. The major highlighting features of these materials are their abundance, biodegradability, and cost-effectiveness [25]. Apart from these benefits, the importance of using these materials for treating effluents is to avoid air pollution caused due to burning of these wastes, which is a common practice in most of the places [20]. Low selectivity for oil is one of the drawbacks of the natural organic adsorbents [26]. Besides, these materials may result in secondary pollution of water due to the release of organic compounds contained within them when used unmodified [1]. One such abundant agricultural waste that can be used as a value-

added product for the application of wastewater treatment is wheat straw. It is a lignocellulosic biomass that possesses abundant hydroxyl groups on its surface. Hence, this material can be modified easily to increase the surface specificity for adsorbing target contaminants [18]. Various chemical modification techniques for lignocellulosic materials with emphasis on increasing hydrophobicity are available. Acetylation [27], Grafting of hexadecyltrimethoxy silane [28] and impregnation of silica (SiO_2) granules [20] are some of the surface modifications applied on different types of straw.

Free radical polymerization is a widely used technique to induce cellulose powders with properties hydrophobicity, thermal stability, mechanical stability, and ion exchangeability [29]. Nevertheless, it is scarcely explored for modifying agricultural waste materials with lignocellulose. There are very few works where lignocellulosic biomass grafted with vinyl monomers have been used to incorporate properties such as flame retardancy [30] and moisture resistance [31–34]. This is a novel study exploring the combination of an adsorption system consisting of a chemically modified agricultural waste material as an adsorbent and microfiltration system.

1.2 Membrane filtration for oil and water separation

Membrane filtration, particularly microfiltration, has been found to be very efficient for separating oil and water [35]. There is a trade-off between flux and rejection when it comes to conventional polymer membranes [36]. Membranes are classified into four main categories i.e. microfiltration (MF), ultrafiltration (UF), nanofiltration (NF), and reverse osmosis (RO) based on the size of pollutants they reject (Figure 1.1(a)). In terms of cross-section morphology, membranes are divided into two types: anisotropic (asymmetric) and isotropic (symmetric) membranes (Figure 1.1(b)). Some of the examples for anisotropic membrane include composite membranes, integrated asymmetric membranes and supported liquid membranes, and microporous membranes, nonporous dense membranes, and electrically charged membranes are some examples of isotropic membranes [37].

A popularly used technique for preparing asymmetric porous polymeric membranes is non-solvent induced phase separation (NIPS). It is a demixing process bringing about the diffusion of the solvent into the non-solvent in a coagulation bath resulting in the formation of a porous structure

[12]. The intrinsic oleophilic property of conventional polymeric membranes can be overcome by endowing the membrane materials with hydrophilic properties through blending with additives such as nanofillers, surfactants, and polymeric additives, surface coating with hydrophilic layers, and surface grafting [11,36]. Numerous studies have used blending as a technique to incorporate hydrophilic additives, copolymers, and nanoparticles to enhance permeation and fouling resistivity since it is a versatile process. Polyvinylpyrrolidone (PVP) is commonly used as an additive for polyethersulfone (PES) and polysulfone (PSF) porous membranes. Matsuyama et al., 2003 utilized PVP while casting a PSF membrane. A highly porous spongy structure was obtained by using PVP of higher molecular weight and lower diffusivity [38]. In another work by Helali et al., 2020, PAI microfiltration membranes were prepared by the NIPS technique by adding PVP and poly (ethylene glycol) (PEG). The PVP and PEG were found to be extremely helpful in achieving an oil removal efficiency as high as 98% at a high permeation rate of 210 $Lm^{-2}h^{-1}$ [35]. Yan et al., 2006 reported an increase in the flux because of the increase in efficient filtration area due to the addition of as a result of the addition of hydrophilic Al_2O_3 nanoparticles [39].

1.3 Liquid-solid mass transfer by adsorption

A mass transfer process reduces the concentration of a given component in one stream to increase the concentration in another phase. The transfer ceases when equilibrium prevails. The basic principle of any mass transfer process can be represented by [40]:

$$r = -\mathrm{D_m}\frac{\partial \mathrm{C}}{\partial \mathrm{x}} \qquad (1.1)$$

where, r is the rate of mass transfer per unit time ($ML^{-2}T^{-1}$), D_m is the co-efficient of molecular diffusion in the x-direction (L^2T^{-1}), C is the concentration of constituent being transferred (ML^{-3}), and x is the distance (L).

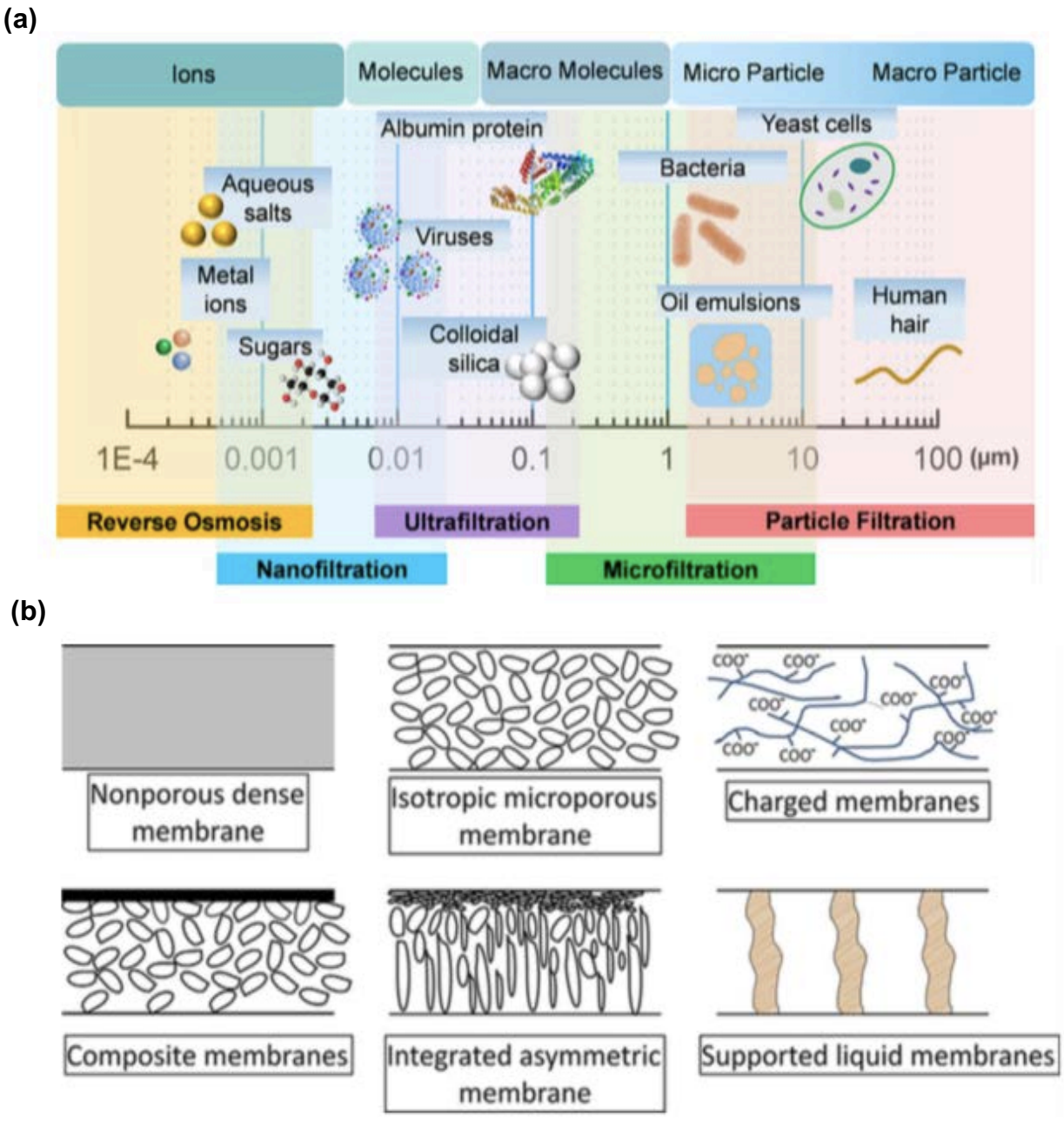

Figure 1.1 Schematic representation of the classification of membranes (a), and classification of membranes based on their morphology (b). Figures are reprinted with permission from [41] and [37].

1.3.1 Mechanism of adsorption

The four main definable steps of adsorption include [29,42]:

a. Bulk solution transport: the adsorbate flows through the bulk liquid by advection and dispersion to the fixed film of liquid surrounding the adsorbent.

b. Film diffusion transport: the adsorbate diffuses into the entrance of the adsorbent through the stagnant liquid film.
c. Pore transport: molecular diffusion through the pore liquid of the adsorbate.
d. Adsorption: the final step where the adsorbate adsorbs on the available adsorption sites.

Adsorption forces include dipole-dipole interactions, point charge, and a dipole, point charge-neutral species, and hydrogen bonding, to name a few. The adsorption process involving intramolecular bonding interactions such as covalent bonding is considered to be chemisorption. The remaining processes involving intermolecular interactions are referred to as physisorption [43,44].

1.3.2 Batch mode of adsorption

The mass balance equation for batch study in which a known quantity of adsorbent is added to the bulk liquid to understand its behavior at equilibrium is given by [40,45]:

Amount of reactant adsorbed within the system	=	Initial amount of reactant within the system	-	Final amount of reactant within the system

$$\text{i.e., } q_e M = VC_o - VC_e \qquad (1.2)$$

where, q_e is the adsorbent phase concentration after equilibrium in mg adsorbate/g adsorbent, M is the mass of adsorbent in g, V is the volume of liquid in the reactor in l, C_o is the initial concentration of adsorbate in mg/l, C_e is the final equilibrium concentration of adsorbate after absorption in mg/l.

Adsorption isotherms aid in determining the mass of reactant adsorbed per unit mass of the adsorbent. The resulting function of the amount of adsorbate adsorbed as a function of concentration and constant temperature is called as 'adsorption isotherm'. A common protocol to develop isotherms is to react a given amount of adsorbate in a fixed volume of liquid with varying amounts of the adsorbent. The loading behavior of the adsorbent as a function of adsorbate concentration in the aqueous phase is analyzed by well-reported models such as Langmuir and Freundlich [33,46].

1.3.3 Langmuir isotherm

This mathematical model is defined for monolayer adsorption, i.e., chemisorption as [47,48]:

$$\frac{x}{m} = \frac{\mathrm{abC_e}}{1 + \mathrm{bC_e}} \qquad (1.3)$$

where, *x/m* is the mass of adsorbate adsorbed per unit mass of adsorbent in mg adsorbate/g adsorbent, *a*, *b* are empirical constants, C_e is equilibrium concentration in adsorbate after adsorption, mg/l.

The main assumptions on which the isotherm is based on are: (a) Adsorption sites possess the same energy, and the numbers of adsorption sites remain constant (homogenous surface), and (b) Adsorption is reversible. Therefore, at equilibrium, the rates of adsorption and desorption are considered the same. A plot of x/m versus C_e is used to obtain the parameters.

1.3.4 Freundlich isotherm

Freundlich model is a more comprehensive isotherm and deals with both homogenous as well as heterogeneous surfaces. In addition, the model applies for multilayer adsorption, i.e., physisorption [47,48]. Expression of this model is:

$$q_e = \mathrm{KC_e^{\frac{1}{n}}} \qquad (1.4)$$

where, *K* is Freundlich constant related to adsorptive capacity, *n* is an empirical value which is a function of the heterogeneity degree of the adsorbent.

1.3.5 Continuous mode of adsorption and mass transfer zone

The continuous mode of adsorption is commonly studied using a column setup. It is known to be highly efficient than batch mode specifically for understanding the suitability of adsorbents for large scale applications such as industries. The concentration gradient between the adsorbent and the bulk liquid is continuous in this mode. Another important factor that makes the analysis in a continuous mode more critical and reliable is the concentration of the bulk liquid. It decreases steadily in batch mode, whereas it remains relatively constant in continuous mode. A plot of effluent concentration as a function of time or volume of effluent gives the breakthrough curve [49].

The area of adsorbed filter bed in the column where adsorption occurs is referred to as the Mass Transfer Zone (MTZ) [50]. As the top layers of the bed (initial MTZ) gets saturated with the contaminants, the MTZ moves down the bed until a breakthrough occurs. Typically, the breakthrough point is considered to be the one at which the effluent concentration is 5% of the influent concentration. The length of MTZ is a function of characteristics of the adsorbent as well as the hydraulic loading rate [51]. The rate-limiting step of the adsorption process is based mainly on the adsorption mechanism. Accordingly, the shape of the breakthrough curve is a function of the adsorption mechanism and thus the rate-limiting step. For the case of physical adsorption, the rate-limiting step will be one of the diffusion transports steps. On the other hand, i.e., for chemical adsorption, it will be the adsorption step itself. In addition, the size of adsorbent particles, column geometry, operating conditions, pH, influent concentration, and nature of the adsorbent also play an important role [52].

1.4 Wheat straw as an adsorbent

Wheat straw is a lignocellulosic biomass in the form of plant material. It is a renewable and geographically well-distributed crop. The global annual production of wheat straw is as high as 529 million tons [53]. Similarly, according to an article in Canadian Geographic in 2016, approximately 20 million tons of unused wheat straw is produced every year in Canada. The main components of wheat straw are cellulose (34-40%), hemicellulose (30-35%), and lignin (14-15%), respectively [54,55].

The lumen in the straw structure has voids, and the layer below the epidermis consists of tube-like conducting tissues called the vascular bundles [54]. Cellulose, a long chain of glucose (ß (1-4)-linked) molecules, is the primary component of the cell wall. Hemicellulose is a polysaccharide responsible for the formation of cross-links between cellulose fibers, microfibrils, and lignin. Lignin acts as a cellular glue and is mainly responsible for providing compressive strength to the plant fibers as well as stiffness to the cell wall [56]. As a result, the presence of both hydrophilic and hydrophobic components makes the straw sparingly soluble in water [27].

1.5 Free radical graft polymerization

In recent years there has been a great practical interest in modifying natural polymers due to their abundance and number of attractive properties such as plenty of hydroxyl groups. Blending, grafting, and curing are the three important techniques available to modify polymer properties. Blending involves the formation of a physical mixture of polymers while curing forms a coating on the substrate by physical forces. Grafting, on the other hand, results in the covalent bonding of the monomer onto the polymer chain [57]. Chemical, radiation, photochemical, plasma-induced, and enzymatic grafting are some of the well-known grafting methods. Among these, the graft polymerization by chemical modification is a facile way to tailor desired material properties to specific end uses without significantly altering the natural properties [58]. Free radical polymerization in chemical redox systems is a highly efficient and promising technique for grafting vinyl monomers. This technique has been extensively used to incorporate desired functionalities into lignocellulosic materials [32]. Using ceric ion for initiating the graft polymerization is very practical and promising, particularly for inducing wetting properties as well as to achieve enhanced adhesion [59]. Ceric ion, an inorganic metal ion, initiates free radical formation and tends to promote grafting mainly in the surface regions. In addition, grafting in a heterogeneous medium takes place mainly in the amorphous regions of cellulose, and hence the crystallinity of cellulose remains unchanged, with modest changes in the mechanical properties. This is because the mechanical properties are mainly governed by the crystalline morphology [59].

The macrocellulosic radicals initiated by the chemical redox systems are temperature sensitive and short-lived [60]. The mechanism of grafting, when the ceric ion is used as an initiator, involves the formation of a short-lived radical on either carbon C2 or carbon C3 of cellulose after cleavage of the anhydroglucose ring between them. The carbon on which the radical is not formed undergoes oxidation. The propagation of the polymer chain will be initiated as a result of a reaction between the radical and the monomer will be terminated by a reaction with Ce^{4+} of the carbon with radical and formation of Ce^{3+}. The reaction below shows the free radical formation [61].

$$Ce^{4+} + R_{polymer}OH \rightarrow complex \rightarrow R_{poly}O^{\cdot} + Ce^{3+} + H^{+}$$

$$R_{polymer}O^{\cdot} + M \rightarrow R_{cellulose}OM^{\cdot} \rightarrow R_{polymer}OMM^{\cdot}$$

When vinyl monomers are used in the solution phase, the morphology and molecular orientation of cellulose, as well as the extent and rate of grafting, becomes a function of the composition of the solution. This is most commonly referred to as the Trommsdorff-Norrish effect, also called gel effect or auto-acceleration [60]. The phenomenon causes a strong deviation in the classical mechanism behavior of a monomer, such as methyl methacrylate. This, in turn, rapidly increases the conversion and molecular mass of the polymer produced. The viscosity of the reaction solution plays a major role in causing the auto-acceleration reaction. Chain termination, as explained before, is a very rapid reaction occurring at high frequencies (about 1 in 10^4 collisions). The increased viscosity of the reaction due to the increase in the concentration of previously formed polymer, in addition to the restriction of Brownian motion of the larger molecules in the highly viscous solution, drastically reduces the collisions between the free radical chains [62]. Hence, diffusion limits the rate of termination. The temperature of the reaction and rate of stirring by the reaction solution are two highly significant parameters that need to be optimized in a heterogenous free radical reaction to avoid the gel effect along with the formation of a homopolymer [63].

1.6 Literature Review

Chemical modification of wheat straw is highly necessary to treat chemically stabilized oil-water emulsions. The raw wheat straw has displayed satisfactory performance only in the removal of floating oil [64]. In the literature, many studies are available on utilizing chemically modified lignocellulosic biomass for dye removal and heavy metal removal by ion exchange. Cationic surfactants such as hexadecyl trimethyl ammonium bromide have been used to remove anionic dyes like congo red [17]. Cationic surfactant hexadecyl pyridinium chloride monohydrate has been used to enhance the oil sorption capacity of wheat straw. In a study [27], acetylated rice straw was modified by treating straw with acetic anhydride with and without tertiary amine catalysts in a solvent-free treatment system. The catalysts facilitated the increase in weight percent gain of the sample by approximately 4%. The adsorption of oil was as high as 24 g of oil/g of straw. However, the potential of acetylated wheat straw was only tested for the removal of floating oil, focusing on the application of oil spill cleanup. According to our knowledge, there is only one study to date on synthesizing poly(methyl methacrylate) grafted rice straw (PMMA-g-RS) [30]. The authors mainly focused on analyzing the thermal behavior, tensile properties, and flame retardancy of the sample in order to use it as a roofing material. The PMMA-g-RS was fabricated using

$CuSO_4$/glycine/ammonium persulfate in aqueous medium for two cases with and without the addition of sodium silicate (SS). The modified PMMA-g-RS/SS composite was found to have high tensile strength of 45.7 N/m^2. The water absorbency percentage of the modified sample was as low as 25%.

In another study, a superhydrophobic/superoleophilic corn straw fiber was fabricated for oil spill removal. The fibers were impregnated with SiO_2 granules. In addition, heptadecafluoro-1, 1, 2, 2-tetradecyl trimethoxysilane was used as a coupling agent to graft with SiO_2 particles. More importantly, the fibers were pre-treated with 0.5 wt% NaOH and 30% H_2O_2 to extract resins and other impurities on the straw surface. This helped in obtaining a large number of exposed hydroxyl groups on the fiber surface, thereby increasing the percentage grafting of SiO_2 as well as hydrophobicity [28]. Graft polymerization, in contrast to other modification techniques, helps in the formation of an ester bond between cellulose and PMMA with exceptionally high hydrophobicity along with chemical, mechanical, and thermal stability.

1.7 Objectives

In this thesis, a thoughtful contribution is being made to the area of oily wastewater treatment and solid waste management. One of the abundant agricultural waste biomasses, wheat straw, is being utilized to pre-treat the microfiltration feed. Herein, the adsorption behavior of the biodegradable PMMA-g-WS is studied systematically in both batch and continuous modes. Therefore, this thesis provides a complete idea about the efficiency of this material in terms of its equilibrium adsorption capacity, breakthrough time, chemical stability, and recyclability. Polyamide and polyamide amorphous polymer with outstanding thermal, mechanical, and chemical properties and highly polar additive PVP has been used to fabricate microfiltration membranes. Since traditional polymeric membranes are highly prone to fouling by oil, the effect of pre-treatment by adsorption using chemically modified wheat straw was analyzed on the performance of commercial membranes as well.

The main objective of the research is to develop a novel hybrid agricultural waste-based adsorption and microfiltration system for oil and water separation. The hydrophobicity of wheat straw was improved by grafting a methyl methacrylate by free radical graft polymerization technique and

synthesis of the PAI membrane by phase inversion technique. The goal was achieved in two phases:

i. Investigation of the equilibrium adsorption capacity in batch mode: The effects of initial oil concentration, adsorbent dosage, and contact time were investigated. Adsorption isotherms were applied to determine the equilibrium adsorption capacity as well as the nature of adsorption.

ii. Investigation of the kinetics of adsorption and breakthrough time: This evaluation was performed in a continuous flow column setup. The dynamic equilibrium performance and reusability of PMMA-g-WS for the treatment of oil-in-water emulsions were evaluated. Later, the system was integrated with microfiltration using both PAI and commercial polymeric membranes.

    The performance of the membranes with and without pre-treatment of different concentrations of oil emulsions was analyzed and compared to obtain insights on the effect of pre-treatment on flux decline and flux recovery and hence the membrane reusability.

1.8 Thesis outline

Chapter 1 of the thesis provides an overview of the importance of treating hydrocarbon containing waste streams, conventional methods used for separating oil and water, and their drawbacks have been discussed. The significance of membrane filtration in separating emulsified oil and the need for a pre-treatment system such as adsorption and some of the fundamental aspects of both adsorption and membrane filtration has been included. The chapter also provides insights on some of the research studies relevant to oil and water separation by chemically modified lignocellulosic materials, phase inversion membranes, and the combination of membrane filtration with different preliminary treatment systems.

Chapter 2 is on the preparation of PMMA grafted wheat straw by free radical graft polymerization in a heterogeneous medium using CAN as an initiator to increase the hydrophobicity of the material. The equilibrium adsorption study and kinetic studies in batch mode to determine the adsorption capacity and rate of adsorption are the main highlights of this chapter.

Chapter 3 is on the application of integrated PMMA-g-WS in the continuous mode of adsorption and the PAI membrane in the dead-end mode for efficient separation of oil and water. The breakthrough curves of adsorption for different oil concentrations and reusability of the PMMA-g-WS has been analyzed. The performance of PAI and commercial polymeric membranes were compared for treating oil emulsions with and without pre-treatment. The permeation and fouling resistance of both the membranes were systematically analyzed.

Chapter 4 provides a summary of the major findings, along with a brief discussion. In addition, based on some important observations/understandings during the course of study, some ideas that can be incorporated in the future have been laid out.

Chapter 2: Enabling the agricultural waste wheat straw for the economical and eco-friendly treatment of oily wastewater by simple modification with poly(methyl methacrylate)

2.1. Introduction

Water pollution due to the influx of wastewater originated from industries or other point and nonpoint sources of contaminations has always been a global concern, which is augmented by today's rapid growth in population and their increasingly luxurious lifestyle. Oily wastewater discharged from oil/gas and petrochemical industries, commonly termed as produced water, poses a major threat to water bodies since it carries several toxic and carcinogenic compounds such as benzene, phenol, and polycyclic aromatic hydrocarbons (PAHs) that can take a death toll on aquatic lives. The low specific gravity of oil results in the formation of an oil film on the surface of the water. One of the serious implications of the formation of oil film on the water is ecological hypoxia. The impedance of solar light penetration by the colored PAHs floating on the water can also obstruct the photosynthesis process in algae and aquatic plants, leading to an imbalanced ecosystem. Apart from that, the discharge of oily wastewater on land can potentially contaminate soil, groundwater, and air. For countries such as Canada, which holds the world's third-largest oil reserves and produces approximately 1.2 million barrels of conventional oil per day, the development of efficient and economic oily wastewater treatment technology is pivotal for the sustainable growth of its oil industry. Plenty of value-added schemes can be considered to reuse the reclaimed water, including industrial reuse (e.g., cooling towers and boiler makeup water), urban reuse (e.g., golf courses and recreational field irrigation), agricultural reuse, recreational and landscape impoundments, snowmaking, and environmental reuse (e.g., wetlands, river or stream flow augmentation). The maximum oil concentration limit in the reclaimed water should be very low or almost nil for various applications. For example, the US EPA (the United States Environmental Protection Agency) limits the oil concentration in the range of 0.2-1 ppm for boiler operations. Canadian regulations also require the oil concentration to be <5 ppm before the discharge of the oily wastewater into water bodies [4].

The past few decades have witnessed a significant advancement in process and technology development in the essence of exploring efficient, economic, and environmentally friendly oily wastewater treatment techniques, some of which include adsorption-based filtration [65], dissolved air flotation (DAF) [66], gravity coalescer [67], advanced oxidation process (AOP) [64], electro-coagulation and electro-oxidation [68], activated sludge process [8], and membrane separation [69]. However, any individual technique is not sufficient to achieve high-quality of the reclaimed water and is chemically and energetically demanding and time-consuming. Membrane separation is a stand-alone technique for the separation of any type of contaminants, irrespective of their size and/or chemical characteristics, yielding high-quality reclaimed water with minimal chemical footprint. However, membrane fouling caused by a high concentration of oil, organic matter, and microorganisms present in oily wastewater streams dramatically reduce the life span of the membrane and require frequent chemical cleaning, which diminishes its advantages. Therefore, a hybrid treatment technique integrating a pre-treatment system along with and membrane separation is found to be practical. Membrane bioreactor, for example, is widely used as a hybrid technique for the treatment of municipal and industrial wastewater [70], [71,72]. However, the biological treatment based on the activated sludge process involved with membrane filtration needs longer stabilization times. Also, the biomass present in the system may cause extensive fouling of the membrane surface [73]. A study on the treatment of oily wastewater using a hybrid system consisting of a coagulation process and a membrane filtration process demonstrated a robust system with high effluent quality [5]. Pre-treatment of the effluent using the coagulation process before subjecting to membrane filtration reduced the fouling load on the membrane allowing a high-throughput filtration capacity. It also allowed the production of a high-quality permeate featuring oil removal efficiencies of 98.5% and reduction in chemical oxygen demand (COD) by 95.2%. However, the chemical coagulation is a tedious process and adds further chemical footprint to the hybrid process. Meanwhile, electrocoagulation (EC) and a nanofiltration (NF) membrane integrated hybrid process was used to treat bilge water containing oil and grease [13]. While EC alone provided only ~50% lowering of COD in the treated water in a 90-minute treatment time at applied voltage of 10.45 V and pH = 8, the integrated hybrid system lowered the COD up to 26%. However, electrocoagulation as a pre-treatment technique is not economically and technologically feasible for large scale applications.

The adsorption process is a promising pre-treatment technique since it is a simple, sustainable, cost-effective process. It is also found to be efficient in removing free, dispersed, and emulsified oil. The adsorption-based technique is also suitable for the treatment of diluted effluents [18] [74]. The most common traditional adsorbent used for oil-water separation is activated carbon (AC). Activated carbon systems, however, are not economical and require rigorous regeneration of spent activated carbon due to its microporous structure [19]. Apart from that, its major drawback would be the carbon footprint being seriously destructive for the environment. One estimation shows that the consumption of each kg of AC can release approximately 0.7 kg of carbon dioxide with the embodied energy of around 70 MJ [75]. Other synthetic high-performance adsorbents such as graphene-based materials and carbon nanotubes are complicated and expensive to prepare and also characterized by their high carbon footprint [76].

In the context of exploring cheaper, environmentally benign, and low carbon-emitting adsorbents, recent research focus has largely been subjected to utilizing renewable natural organic materials, such as agricultural by-products, as an alternative to traditional adsorbents. It is undoubtedly wise to develop processes that can resolve diverse issues at the same time. One such process development would be utilizing a waste by-product to treat another waste since it would simultaneously resolve the challenges of waste management involved in both cases. Agricultural wastes used as adsorbents for treating hydrocarbon-containing effluents include rice husk [21], wheat straw, cotton fiber [23], and banana peels [24] to name a few. The outstanding advantages of using such lignocellulosic biomasses are their abundance, biodegradability, and cost-effectiveness. Apart from these benefits, the importance of using them for treating effluents is to avoid air pollution caused due to burning of these wastes, which is a common practice in most of the places [77]. Another notable advantage of these biomasses is their low carbon footprint [75]. On the other hand, the low absorptivity of oil is one of the major drawbacks of these natural organic adsorbents [26]. These materials can also result in secondary pollution by releasing their constituent organic compounds when used in the pristine form [1]. Therefore, it is necessary to explore simple chemical modification methods that can enhance the oil absorptivity and prevent secondary pollution while retaining the cost-effectiveness and biodegradability.

Among the variant of natural bio-adsorbents, wheat straw is unique due to its highest abundance, relatively higher structural stiffness, and well-studied chemical structure and surface reactivity. The structural stiffness of wheat straw makes the pulverization process easy to obtain desirable particle sizes. The availability of information on its chemical structure and surface reactivity facilitates the design of structural and surface modification methods that are suitable for adsorbing target contaminants [18]. Numerous reports have appeared on utilizing chemically modified straw for heavy metal removal [78] and dye removal [79]. A few studies also demonstrated the application of chemically modified wheat straw for oil adsorption. Some of the common surface modification methods applied on straw for oil adsorption include surfactant modification, acetylation [27], hexadecyl trimethoxy silane modification [80], and impregnation of silica (SiO_2) granules by heptadecafluoro-decylalkyl trimethoxysilane coupling agents [20]. The surfactant modification is based on the electrostatic interaction of the cationic ends of the surfactants and the negatively charged sites of the adsorbent surface, leaving the surfactants susceptible to leaching into the permeate water. Meanwhile, the acetylation and silane coupling reactions form ester and silyloxy bonds, respectively. These bonds are susceptible to hydrolysis under acidic or basic pH, making these surface modifications undesirable for the long-term treatment of alkaline oily wastewater, such as oil-gas produced water having pH in the range of 9-11. These reactions also required a large excess of chemicals that increased the chemical footprint. The fluoro silane modification for the SiO_2 impregnation approach also alters the biodegradability of the straw, and the use of halogenated compounds should be avoided since these are deleterious for the atmosphere. In this context, it is important to explore surface modification methods that can retain the original properties of the waste biomass. Polymer grafting by free radical polymerization is a popular technique since it is straightforward, chemically less demanding, cost-efficient, and does not alter the original properties of the material being grafted [60,81]. Grafting of various polymers on cellulose through free radical polymerization is widely used to induce hydrophobicity, thermal stability, mechanical stability and ion exchange properties [82]. However, free-radical mediated polymer grafting is scarcely explored for the modification of lignocellulosic biomasses such as wheat straw. Poly(methyl methacrylate) (PMMA) grafting has previously been used to increase flame retardancy [30] and moisture resistance of lignocellulosic biomasses [32,34,48]. Surprisingly, PMMA grafted biomasses (e.g., wheat straw) was not utilized for oil water separation

despite of having relevant favourable properties, such as lower price, hydrophobicity, resistance to acid/base hydrolysis, biocompatibility, and reasonable biodegradability of PMMA.

In this study, PMMA grafted wheat straw (PMMA-g-WS) was explored for the adsorptive pre-treatment process to separate oil from oil-water emulsions. At first, the raw dried straw was mechanically ground into 250-425 μm size particles to increase the adsorptive surface area and to enable tight packing of the adsorption column bed. Then, the straw was pre-treated with alkaline hydrogen peroxide to remove the wax, resins, and lignin. The sub-objectives applying the pre-treatment were: (a) exposing the surface hydroxyl groups that are otherwise covered under the wax layer, and (b) increasing the adsorptivity of oil by creating enhancing the surface roughness. Cerium Ammonium Nitrate (CAN) has been chosen as the reaction initiator since it helps to graft polymers predominantly on the surface and to simplify the modification reaction by allowing it to be performed in an aqueous medium without the use of stringent inert atmospheric conditions such as that required for atom-transfer radical polymerization (ATRP) [17,83]. The success of PMMA grafting was assessed by attenuated total reflection-Fourier transform infrared (ATR-FTIR) spectroscopy and Energy-dispersive X-ray (EDX) spectroscopy. The percentage of PMMA grafting was evaluated by gravimetric analysis. Surface morphology was evaluated by scanning electron microscopy (SEM). Surface wettability was analyzed by water and oil contact angle measurements, while oil removal efficiency and adsorption capacity were studied by batch oil adsorption experiments. Langmuir and Freundlich isotherms were applied to understand the adsorption mechanism. Finally, adsorption kinetics was studied by applying pseudo-first-order and pseudo-second-order kinetic models.

2.2 Experimental

2.2.1 Materials and Chemicals

Wheat straw was obtained from a farm in the Edmonton area. Methyl methacrylate (MMA) (99%), cerium ammonium nitrate (≥98%), and nitric acid were all obtained from Sigma Aldrich and were used as received. Acetone and methanol used for the purification of grafted material were purchased from Fisher Scientific. Ethanol (95%) used for the regeneration of the spent column was procured from Fisher Scientific. Sodium hydroxide pellets and hydrogen peroxide (30%) used for

the pre-treatment of straw particles prior to grafting were purchased from Fisher Scientific. Diesel oil was obtained from a local fuel station.

2.2.2 Pre-treatment of wheat straw

Wheat straw was pulverized and sieved through 60 and 80 mesh screens to obtain particles in the size range of 250-425 µm. The particles were rinsed ultrasonically with deionized (DI) water, followed by ethanol and DI water washing. Each 4g of wheat straw particles was treated with 100 ml of 0.5 wt% NaOH and 3.5 ml of 30% H_2O_2 [20]. The solution was stirred for 14 h at ambient temperature. The unreacted reagents and by-products were removed by thoroughly rinsing the pre-treated particles with DI water and ethanol. Any excess alkaline residue in the solution was neutralized by adjusting the pH in the range of 6.5-7.0 using 6 mol/l HCl. At last, the pre-treated particles were rinsed thoroughly with DI water and dried at 40 ^{0}C until a constant weight was reached.

2.2.3 Preparation of PMMA-g-WS

The pretreated wheat straw was dispersed in a fixed volume of DI water. The volume of DI water was optimized during the initial reactions with the intention of keeping the amount of solvent as low as possible to disperse the straw particles, maintaining good miscibility of all the reagents, providing favorable reaction kinetics, and facilitating the precipitation of PMMA grafted particles from the reaction mixture which helps the visual preliminary interpretation of the success of the reaction and ultimately eases the purification process. The dispersion was stirred at 70 ^{0}C for 1 h under nitrogen atmosphere. Following that, MMA was added dropwise using a syringe, and the reaction mixture was stirred at 350 rpm. Finally, 10 ml of 2 mmol/l of CAN solution, prepared by dissolving CAN in 0.1 mol/l nitric acid, was added to the mixture and stirred under the nitrogen atmosphere. The weight ratio of WS/MMA was varied from 0.75 to 3.65 in order to optimize the amount of MMA required for the effective grafting of PMMA. The mixture was cooled down to room temperature, and the grafting was terminated by pouring the mixture into excess methanol solution, followed by washing the precipitated PMMA-g-WS granules with DI water. The grafted particles were then dried at 40 ºC until a constant weight is reached. The ungrafted homopolymer

was extracted using acetone in a Soxhlet apparatus. The extracted sample was dried at 40 ºC for 24 hours. The grafting percentage (Gp) was calculated as [84]:

$$Gp = \frac{W_2 - W_1}{W_1} \times 100 \qquad (2.1)$$

where, W_1 is the initial weight of wheat straw particles in g, and W_2 is the weight of PMMA-g-WS particles in g.

2.2.4 Characterization of PMMA-g-WS

The grafting of PMMA was evaluated by comparing the ATR-FTIR (Bruker, Equinox 55) frequencies of PMMA-g-WS with that of raw and pre-treated WS. The surface morphology was analyzed by scanning electron microscopy (SEM), and the elemental composition was determined by Energy-dispersive X-ray (EDX) spectroscopy. The wettability of the samples was analyzed by measuring contact angles by the sessile drop method (Kruss GmbH). The wheat straw samples were pressed and compacted using an FTIR pellet press at room temperature to obtain pellets with approximately 5 mm diameter [85]. The pellets were firmly fixed on a glass side using double-sided tape. A 2µl droplet of water or oil (diesel) was placed on the sample surface using a syringe, and the measurements were taken at three different points to obtain an average value. The surface area of the pristine, pre-treated, and PMMA-g-WS particles was analyzed using Brunauer-Emmett-Teller (BET) theory, and pore size distribution was analyzed with DFT (Density Functional Theory) by outgassing the samples with nitrogen at 150 °C for 2 hrs (Quantachrome Autosorb iQ).

2.2.5 Preparation of oil-in-water emulsions

Three different concentrations (100, 200, and 300 ppm) of oil-in-water emulsions were prepared by placing 100, 200, and 300 mg of diesel in 1 L of DI water followed by probe sonication (Cole-Parmer ultrasonic processor) for 15, 25, and 35 min respectively at 60% amplitude in pulse mode (3s on and 1s) [86]. Following that, the solutions were homogenized (Fisherbrand™ 150) at 10,000 rpm for 15 minutes. The stability of the emulsions was assessed by visually monitoring for 24 h.

2.2.6 Emulsion characterization

Dynamic light scattering technique (DLS, ALV/CGS-3 Compact Goniometer) was used to determine the size distribution of oil droplets in the emulsion. The oil emulsion of 100 ppm concentration was found to be monodisperse with a droplet size of 0.47 µm. The monodispersity of the solution is believed to be because of the low concentration of oil, in addition to the large specific surface area of the oil droplets due to their sub-micron size [87].

2.2.7 Batch adsorption study

Oil removal efficiency and adsorption capacity of the pristine, pre-treated, and PMMA-g-WS were studied by batch adsorption experiments. Three different variables considered for the adsorption study were the initial oil concentration, the adsorbent dosage, and the contact time. The experiments were carried out by varying the adsorbent dosage from 5 to 25 mg for each initial oil concentrations of 100, 200, and 300 ppm, respectively. Centrifuge tubes with a capacity of 50 ml were filled with 40 ml of emulsion and mixed at a constant shaking speed (160 oscillations/min) using a mechanical shaker (Eberbach 6000), for a total time of 60 minutes. The PMMA-g-WS samples were then centrifuged at 1000 rpm, and the remaining oil concentration was analyzed by measuring the scattering at 290 nm with a UV-visible spectrophotometer. A control sample containing only the emulsion was also tested.

The adsorption capacity and oil removal efficiency were calculated using the formulas [86]:

$$q_t = \frac{(C_0 - C_t)\,V}{W_g} \qquad (2.2)$$

$$RE = \frac{C_0 - C_t}{C_0} \times 100 \qquad (2.3)$$

where, C_0 is the initial oil concentration (ppm), C_t is the oil concentration at time t (ppm) after adsorption on WS samples, V is the volume of emulsion (ml), and W_g is the mass of adsorbent (mg).

2.2.8 Adsorption isotherms

Adsorption isotherm models were used to graphically represent the equilibrium relationship of the adsorption process. It describes the amount of oil being adsorbed by the WS samples as a function of adsorbent concentration at a constant temperature.

2. 2.8.1 Langmuir isotherm

This model is mainly defined for monolayer adsorption [47] where the following assumptions are considered: (a) adsorption sites possess the same energy, and the number of adsorption sites remains constant (homogenous surface), and (b) adsorption is reversible. Therefore, at equilibrium, the rates of adsorption and desorption are assumed to be the same. The linearized form of the Langmuir equation is given by:

$$\frac{C_e}{q_e} = \frac{1}{q_m b} + \frac{C_e}{q_m} \qquad (2.4)$$

where, C_e is the concentration of oil (ppm) at equilibrium, q_e is the value of q at equilibrium (mg), q_m is the mass of adsorbate adsorbed per unit mass of adsorbent (mg adsorbate/g adsorbent), and b is an empirical constant. A plot of C_e/q_e versus C_e is used to determine the mechanism of adsorption.

2.2.8.2 Freundlich isotherm

Freundlich model is a more comprehensive isotherm and deals with both homogenous and heterogeneous surfaces. In addition, the model applies for multilayer adsorption, i.e., physisorption [47]. The expression of this model is given by:

$$q_e = KC_e^{1/n} \qquad (2.5)$$

where, *K* is Freundlich constant related to adsorption capacity, and *n* is an empirical value which is a function of the degree of heterogeneity of the adsorbent. The intercept of the plot of log q_e versus log C_e gives *K* and *n*.

2.2.9 Adsorption kinetics

Pseudo-first order and pseudo-second-order kinetic models are widely applied to understand the behaviors involved in the uptake of pollutants by adsorbents. The experimental data obtained by varying the contact time at five minutes intervals using an initial oil concentration of 300 ppm, WS samples dosage of 5 mg, and shaking speed of 160 oscillations/min were analyzed by plotting a linear fit. The pseudo-first-order kinetic equation in linear form is given by [86]:

$$\ln(q_e - q_t) = \ln q_e - k_1 t \qquad (2.6)$$

where, q_t is adsorption capacity at time t (mg/g), k_1 is the pseudo-first-order rate constant (min^{-1}). The plot of $\ln(q_e-q_t)$ versus t was used to determine k_1.

The pseudo-second-order kinetic equation in linear form is given by:

$$\frac{t}{q_t} = \frac{1}{k_2 q_e^2} + \frac{t}{q_e} \qquad (2.7)$$

where, k_2 is the pseudo-second-order rate constant (g/mg min). A linear fit of t/q_t versus t was applied to obtain k_2 and q_e from intercept and slope, respectively.

2.3 Results and Discussion

2.3.1 Pre-treatment of raw WS and PMMA grafting via radical initiated polymerization

The mechanism of grafting with ceric ion (Ce^{4+}) as an initiator involves the formation of an intermediate complex with the cellulosic units and results in a macrocellulosic short-lived radical on either carbon C_2 or carbon C_3 hydroxyl groups of cellulose (Figure 2.1). The polymeric chains will be incorporated onto the cellulose backbone at these active sites resulting in the formation of the graft copolymer. The propagation of the polymeric chain will be initiated by the reaction between the macrocellulosic radical and the monomer. The reaction terminates when the polymeric radicals react among themselves or react with Ce^{3+}, resulting in the regeneration of active Ce^{4+} species. However, the fibrous cellulose in the WS cell wall needs to be exposed by following a pre-treatment process. Moreover, pre-treatment is also necessary to increase the surface roughness by removing lignin and hemicellulose intercalated between the cellulose fibers. Higher surface roughness and pore volume are essential to enhance the oil adsorption. Lastly, pre-treatment is also required to remove surface adsorbed wax and resins that can leach and lead to secondary pollution during the wastewater treatment process. A simple one-step economical pre-treatment of WS, using a mixture of 0.5 wt% NaOH and 30% H_2O_2, is shown to be effective in serving all the purposes described above [29]. Figure 2.1 shows pre-treatment derived degradation of cell walls, exposure of internal cellulose fibers, and extraction of lignin and hemicellulose.

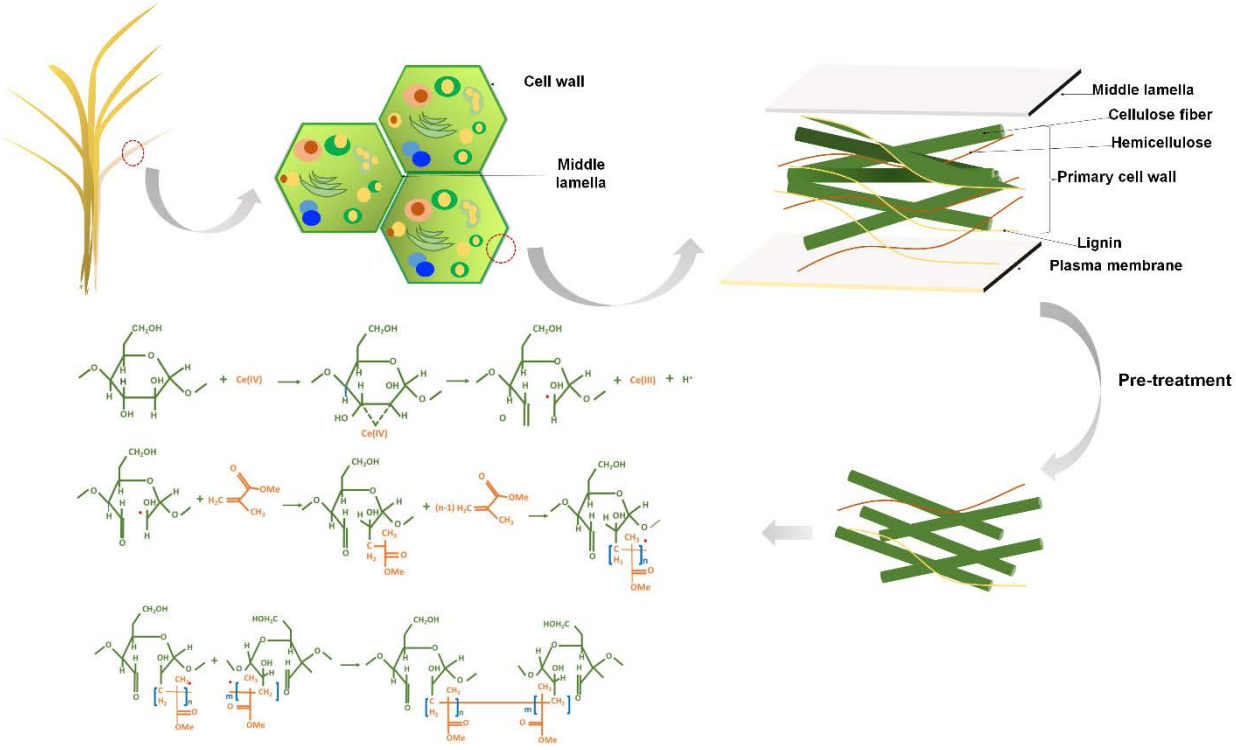

Figure 2.1 Structure of lignocellulosic WS, the pre-treatment process to expose the embedded fibrous cellulose, and the mechanism of graft copolymerization of PMMA on the exposed fibrous cellulose [71].

2.3.2 Optimization of monomer concentration

The significant parameters that influence the grafting percentage (Gp) include reaction time, initiator concentration, monomer concentration, and reaction temperature. The effect of these parameters on the efficiency of CAN initiated polymerization has been extensively studied by many researchers. Therefore, reaction time, temperature, and initiator concentration were chosen from previous literature, and this study focused on the effects of monomer concentration on the grafting percentage of PMMA since the objective was to use the minimum amount of monomer to enhance the cost-efficiency of the straw modification. Moreover, monomer concentration is the predominant parameter that defines the graft percentage of CAN initiated polymerization. The concentration of monomer significantly affects the dilution of macrocellulosic radical sites, miscibility of the reagents, viscosity of the reaction medium, and availability of the monomers in the vicinity of macrocellulosic radicals. The weight ratio of WS/MMA varied from 0.75-3.65, and the highest graft percentage of 127% was obtained for the WS/MMA ratio of 1.25. The increase in the monomer amount from 2.6 ml of MMA to 5 ml and then to 8 ml increased the graft

percentage of PMMA. However, a further increase in the monomer concentration up to 13.3 ml caused a downfall in the PMMA graft percentage. This lowering in the percentage of grafting at high monomer concentration can be associated with the dilution of the WS, increased phase separation between the solvent water and monomer, and the higher viscosity of the reaction medium that ultimately slows down the diffusion of the monomer to the active sites. The WS with the highest PMMA grafting percentage of 127% was used for all relevant characterization and oil adsorption studies.

2.3.3 Characterisation of adsorbents

A concise knowledge of the surface morphology, porosity, microstructure, and chemical composition of an adsorbent is critical for any adsorption study. The BET method is widely used to assess the surface area of non-porous, macroporous, and mesoporous materials with pore width >4nm [88]. The surface area and pore width of all the three samples are presented in Table 2.1. The shape of the hysteresis loops in Figure 2.2 and the pore width values clearly indicate the predominance of mesopores in the straw structure. The International Union of Pure and Applied Chemistry (IUPAC) isotherm type IV(a) and (b), therefore, comes into the picture [43]. The pore width >4nm, as determined by DFT, substantiates this explanation.

The type (IV) isotherms are usually observed for materials with complex pore system. The morphology of the materials shows a highly diverse distribution of pores and hence indicates that the material indeed has a complex porous structure. The shape of the hysteresis loop for pristine straw mostly correlates with type H2(a) hysteresis, since the desorption curve is steep [88], the reason being a wide distribution of pore cavity compared with the neck distribution. The structure of the tubular vascular interconnected vessels with numerous pits at each node (Figure 2.2) justifies this finding.

Table 2.1 BET surface area and pore width of pristine, pre-treated and PMMA-g-WS

Sample	BET surface area (m^2/g)	Pore size (nm)
Pristine	3.84	1.6-6.5, 7-20, 26-32
Pre-treated	2.60	1.6-5, 10-24, 26-34
PMMA-g-WS	2.99	1.6-4, 4-12, 28-32

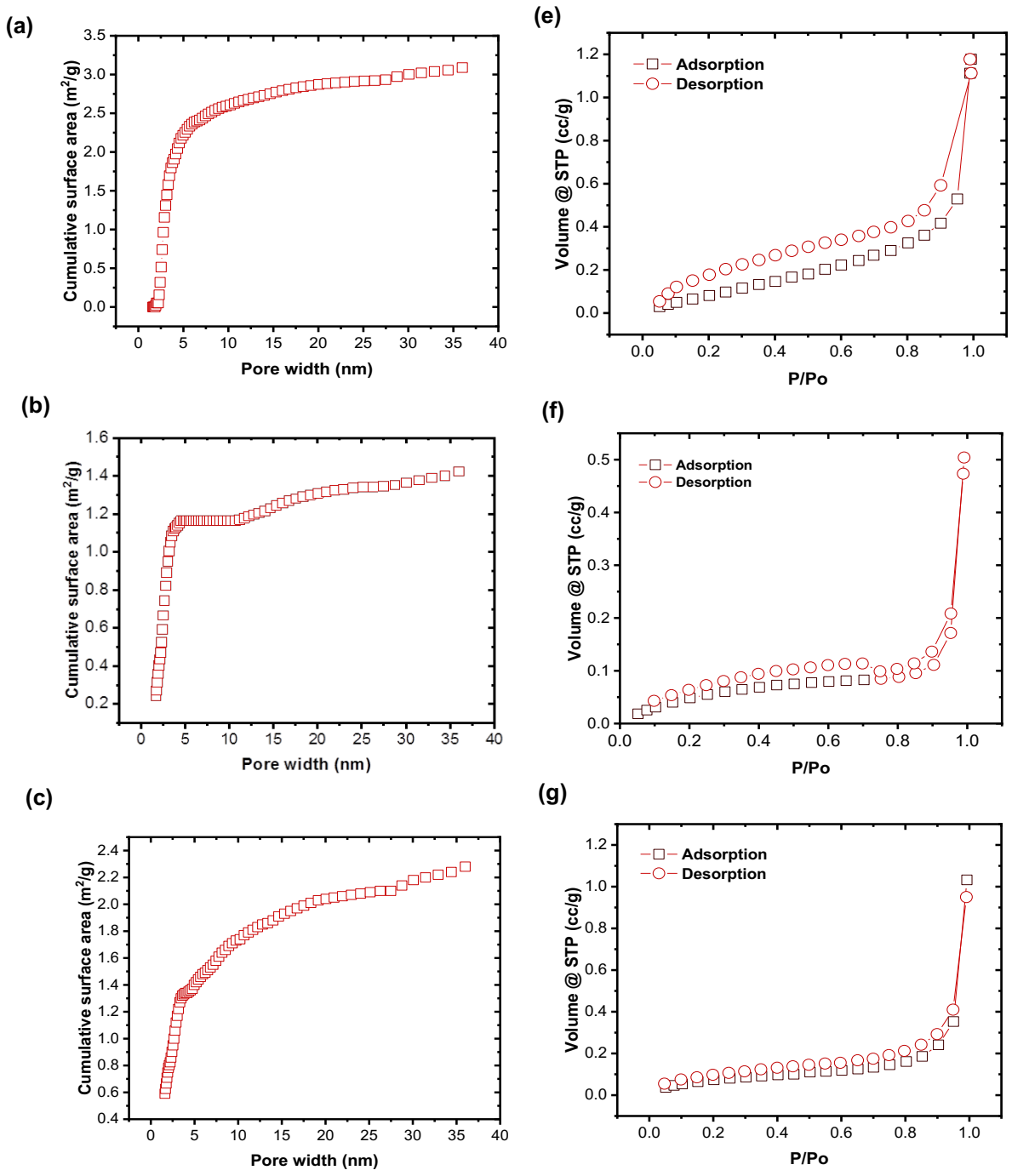

Figure 2.2 Cumulative surface area (a, b, c), and adsorption/desorption curves of nitrogen for pristine, pre-treated, and PMMA-g-WS (d, e, f).

On the other hand, the shape of the DFT results also indicates that the pristine sample has a large number of mesopores compared to the pre-treated and PMMA-g-WS. The hysteresis loop shape for pre-treated and PMMA-g-WS also indicates type H2(a), but with cavitation [89]. This means that the smaller pore size at a certain critical temperature and adsorption is resulting in desorption through cavitation. This can be justified by the fact that the pre-treated and PMMA-g-WS contain numerous micropores along with mesopores in contrast to the pristine straw. Hence, the micron-sized pores are causing cavitation in these samples. The surface area of the samples is in the order pristine>pre-treated>PMMA-g-WS. This trend is mainly believed to be due to the kinetic restrictions associated with the flow of nitrogen into narrowest micropores (<0.45 nm).

Nitrogen is at times inappropriate for analyzing micropores, and also the interaction of nitrogen with non-polar surface functionalities, like in our case, the grafted PMMA, can lead to inaccurate surface area values as these interactions may shift the pore filling pressure of nitrogen to very low relative pressure (P/P_o = about 10^{-7}). Hence, P/P_o does not correlate with the micropore sizes in these cases. Carbon dioxide and argon adsorption are said to be highly efficient in analyzing ultra-micropores and micropore, respectively, due to significantly less interaction with surface moieties and smaller kinetic diameters compared to nitrogen.

The SEM micrographs (Figure 2.3) display the distinctive fibrous microstructures and the surface morphology of the pristine, pre-treated, and PMMA grafted wheat straw. At lower magnifications, the structure of the pristine, pre-treated, and PMMA-g-WS samples looked similar. This indicated that the overall original structure of the wheat straw was retained. The micrographs at higher magnifications clearly displayed the differences between the three samples. While the pristine straw exhibited a homogenous, smooth surface with a hollow tubular structure, the pre-treated straw sample exhibited a loose and fibrous structure with increased porous structure opened along the pore walls indicating that the alkaline hydrogen peroxide pre-treatment was effective to increase the surface roughness and porosity. Note that the internal pore walls of the raw WS is predominantly hydrophilic and used for the transport of water; these pores are, therefore, not accessible to oil due to the limited capillary penetration and needs to be opened from the sides of the pore walls to allow access to oil. The PMMA grafted WS samples exhibited an undulant coarse surface and a mesh-like texture among smoother domains of PMMA, indicating the presence of a

percolating network. Similar observations were reported for grafting PMMA on *Agave americana* fibers [90]. In addition, the magnified SEM image of PMMA-g-WS shows exposed vessels that are a part of the vascular tissue xylem. They are composed of numerous bridging fibrils which conducts water through the plant body. The microporous structure of the PMMA-g-WS is also showcased by the profuse vessel to vessel pitting [91]. The breaking down of PMMA-g-WS into smaller sizes, the formation of percolating network and exposed vessels, and the vessel to vessel pitting are all beneficial for enhanced oil adsorption. The elemental composition of pristine, pre-treated, and PMMA-g-WS is evaluated by EDX analyses (Figure 2.3). The main elements existing in the pristine WS are carbon (C, 35.2%), oxygen (O, 47.1%), and silicon (Si, 17.7%). Carbon and oxygen are originating from basic compositional polymers (i.e., cellulose, hemicellulose, and lignin) of WS as well the wax and resins of the cell walls. Meanwhile, silicon is originating from the abundant silica in the plant cell walls accumulated by the absorption of silicon from the soil [92,93]. In contrast to the pristine straw, the percentage of silicon is negligible in pre-treated straw. This indicates that the alkaline hydrogen peroxide pre-treatment removes the silica from the cell wall, almost completely leaving behind the empty cavities, which are essential for higher oil adsorption capacity [92]. Moreover, the C/O ratio in the pre-treated WS is 1.14, which is very close to the C/O ratio of 1.2 in cellulosic repeating units, meaning that alkaline hydrogen peroxide pre-treatment effectively removed wax, resins, silica, lignin, and hemicellulose leaving mostly the cellulosic fibrous structure. The removal of these materials is essential to eliminate the materials responsible for secondary pollution, expose the reactive surface sites, and increasing pore volumes for oil adsorption. Meanwhile, the C/O ratio in the PMMA-g-WS is twice that in the pre-treated WS, indicating the considerable grafting of PMMA onto the fibrous cellulose backbone; the efficient grafting of PMMA are essential for the hydrophobization of the fibrous cellulose to effectively utilize the exposed surface and pore volumes for the oil adsorption. The observation in the changes in the elemental composition upon PMMA grafting is consistent with a previous study in which PMMA grafted rice straw has been used as a roofing material [30].

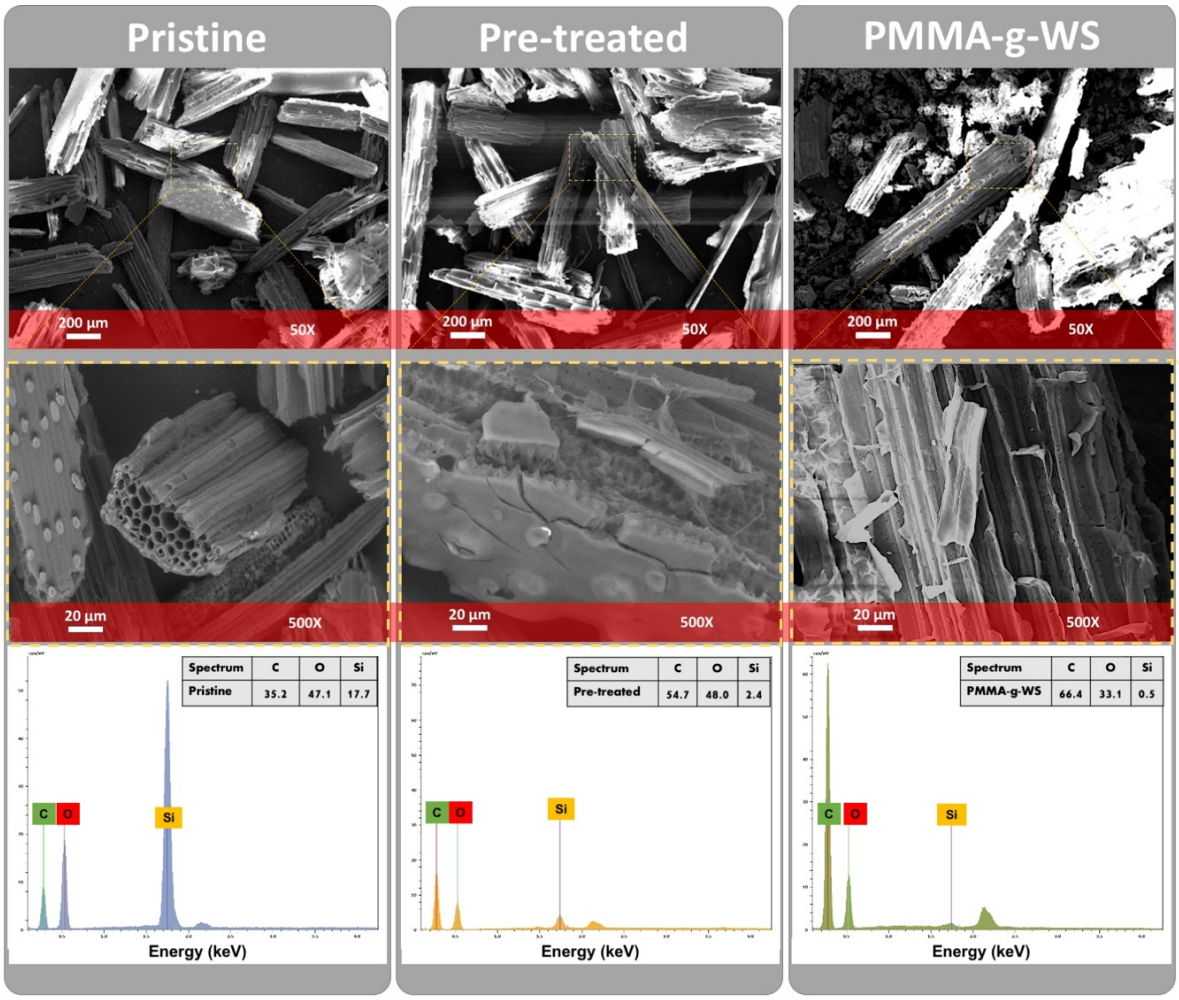

Figure 2.3 SEM micrographs at lower and higher magnifications, and EDX results of pristine, pre-treated, and PMMA-g-WS. The hollow tubular structure of the pristine straw and porous structure with increased surface roughness and loose fibers of pre-treated straw are easily visible. The PMMA-g-WS sample possessed vessels with numerous micropores.

The success of pre-treatment and subsequent PMMA grafting was evaluated by the disappearance of characteristics pristine WS vibration modes and the appearance of characteristics PMMA vibration modes in the FTIR spectrum of pre-treated WS and PMMA-g-WS, respectively (Figure 2.4). The carbonyl (C=O) stretching vibration due to the carbonyl groups of wax, hemicellulose, and lignin around 1750 cm^{-1} in pristine straw is almost absent in pre-treated straw. This can be attributed to the extraction of wax, hemicellulose, and lignin during pretreatment [55]. A dominant peak at 1049 cm^{-1} is for the C-O stretching vibration of the C-O-C ether linkage and C-O-H bonds and the second dominant peak in between 3100-3600 cm-1 is for the O-H stretching vibrations of

the hydroxyl groups of cellulose, hemicellulose, and lignin present in pristine WS. [94]. The intensity of these peaks became more pronounced in the FTIR spectrum of pre-treated WS, further supporting that pre-treatments removed other species leaving the cellulose fibrous structure predominantly since cellulose units contain more OH functional groups and ether linkage than those present in lignin and hemicellulose. Lastly, the intensity of the hydroxyl group's peak declined significantly after grafting of PMMA on the pre-treated sample as a result of their participation in radical creation that reacted with the monomer and the subsequent replacement with PMMA. Moreover, the evolution of new prominent peaks centered at 1720 and 1187 cm^{-1} are assigned to C=O and C-O stretching vibration modes of the ester groups, respectively, which are characteristics vibration modes of PMMA and confirm the success of PMMA grafting.

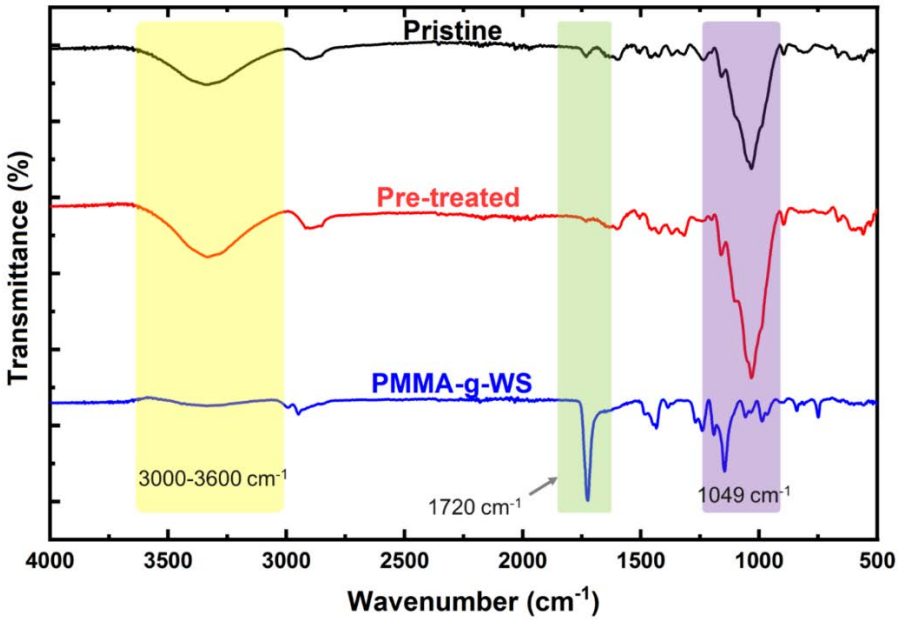

Figure 2.4 FTIR spectra of pristine, pre-treated, and PMMA-g-WS samples.

It is well-known that the surface roughness and surface hydrophilicity/hydrophobicity are the main two influential parameters that determine the surface wettability. Moreover, surface wettability is a crucial parameter for understanding the affinity of the adsorbent to diesel oil as well as water. Meanwhile, the pre-treatment and subsequent PMMA grafting increases the surface roughness and/or hydrophobicity of WS. Therefore, the surface wettability of pristine, pre-treated, and PMMA grafted WS was evaluated by measuring the water and oil contact angles (Figure 2.5).

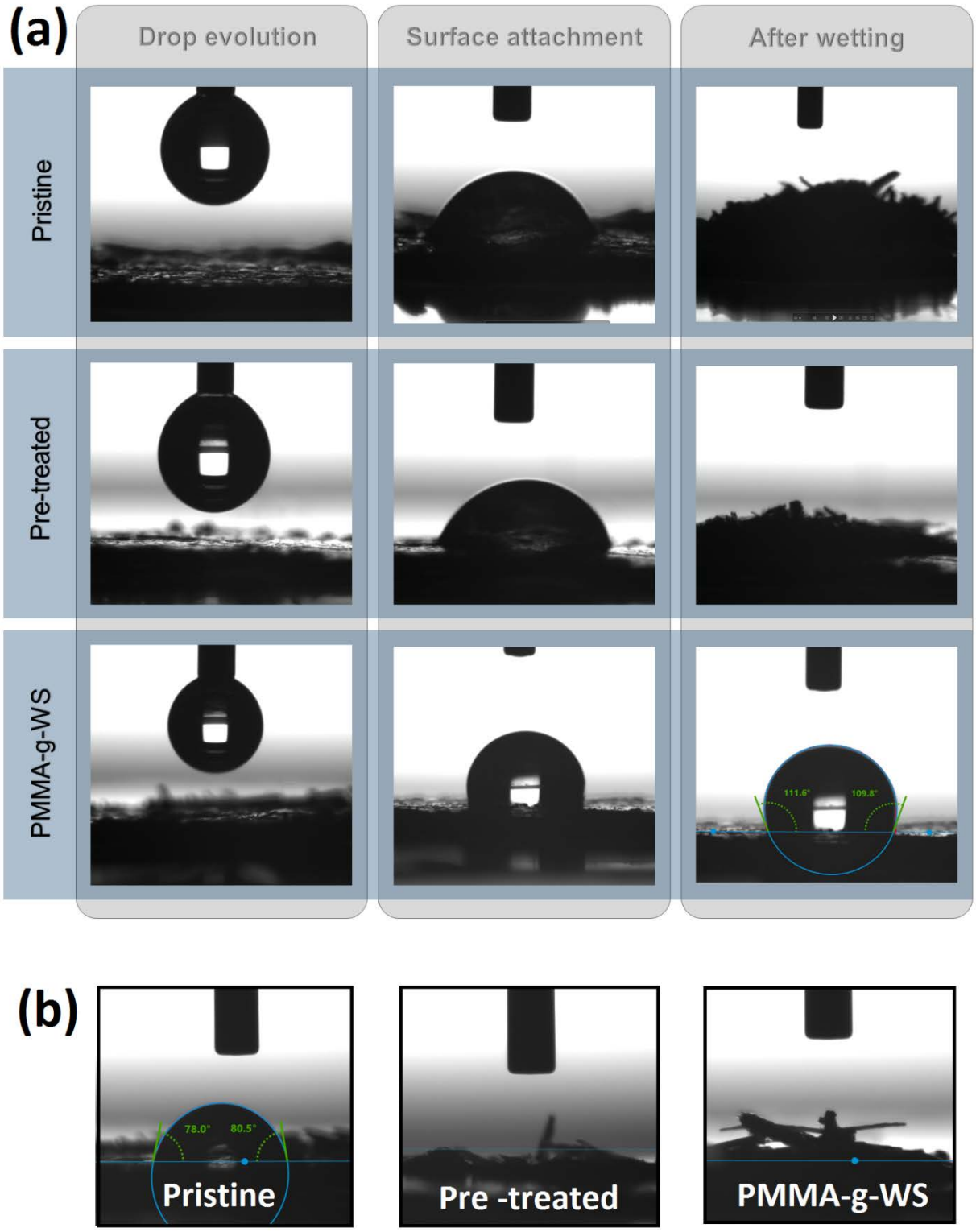

Figure 2.5 Water contact angles of pristine, pre-treated, and PMMA-g-WS in three different time-steps and oil contact angles of all the three adsorbents (b).

Water and oil contact angles for pristine WS were found to be 0° and 79°, respectively. Hydrogen bonding between water molecules and abundant surface hydroxyl functional groups caused full penetration of water droplets into the surface of pristine WS [20]. On the other hand, the hydrophilic surface hydroxyl groups inhibited the adhesion of oil droplets on the surface of pristine WS. Increased porous structures and the presence of macropores resulted in the absorption of both water and oil droplets by the pre-treated WS, although the surface was hydrophilic, which is consistent with similar observations reported previously [20]. In contrast to the pristine and pre-treated WS, the water contact angle of PMMA-g-WS was very high (111°). On the other hand, the oil contact angle for PMMA-g-WS was 0°. The very high-water contact angle and zero oil contact angle confirms extremely high hydrophobicity and oleophilicity of PMMA-g-WS. Therefore, the PMMA-g-WS prepared in this study could be a promising candidate for the adsorptive removal of hydrocarbons from oily wastewater.

2.3.4 Adsorption of oil from oil-in-water emulsion

2.3.4.1 Effect of adsorbent contact time with the oil

A set of experiments were conducted to understand the influence of adsorbent contact time on the oil adsorption efficiency. The experiments were conducted at a constant shaking speed of 160 oscillations/min, initial oil concentration of 300 ppm, and adsorbent dosage of 5 mg at room temperature. The time interval was set to five minutes, and the adsorption experiments were conducted until the final oil concentration in the bulk liquid reached a constant value. A significant amount of oil was adsorbed initially due to the availability of a large number of adsorption sites in the beginning and eventually reached equilibrium, as presented in Figure 2.6. In the case of pristine straw, the equilibrium was reached earlier due to the low porosity of WS and low hydrophobic interactions between the surface of the straw and oil droplets. The overall duration of the adsorption process for pre-treated WS was reasonably higher than the pristine WS due to increased exposure of the porous structure as a result of the alkaline hydrogen peroxide pretreatment, even though the surface of this pre-treated WS is more hydrophilic than that of pristine WS. Hydrophobic interactions between the PMMA-g-WS surface and the oil molecules increased surface roughness and on the WS. The hydrophobic modification of WS pore walls with PMMA hence significantly increased the oil rejection, oil adsorption capacity, and the overall duration of

the adsorption process. The oil removal efficiency of PMMA-g-WS was about 4 times higher than pristine WS and 1.6 times higher than pre-treated WS. The oil adsorption capacity increased from 300 mg/g to 700 mg/g upon pre-treatment and from 700 mg/g to 1000 mg/g upon grafting of PMMA.

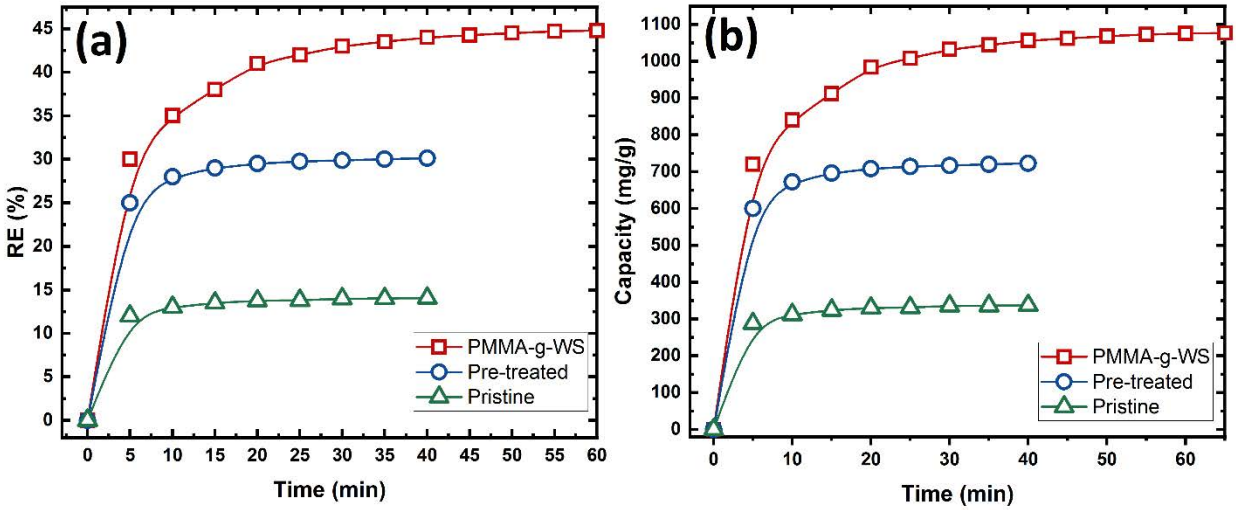

Figure 2.6 Effect of contact time on oil removal efficiency (a), and oil adsorption capacity (b) of pristine, pre-treated, and PMMA-g-WS for 300 ppm initial oil concentration, 5 mg adsorbent dosage, and 160 oscillations/min shaking speed.

2.3.4.2 Effect of initial oil concentration and adsorbent dosage

The effect of different adsorbent dosages and the oil concentration was studied by varying the amount of PMMA-g-WS from 5 mg to 25 mg for initial oil concentrations of 100, 200, and 300 ppm. The contact time and shaking speed were kept constant at 30 minutes and 160 oscillations/min, respectively. As shown in Figure 2.7 a, the adsorptive oil removal efficiency (RE) increased linearly with the increase in adsorbent dosage, and it was higher for 100 ppm oil concentration. The reason behind higher removal efficiencies at a higher adsorbent dosage and lower oil concentrations is the availability of higher adsorption sites for oil accumulation sufficient to accommodate all the oil present in the bulk solution. In contrast to the increase in oil removal efficiency, the adsorption capacity of PMMA-g-WS decreased with an increase in adsorbent dosage, and a decrease in oil concentration. The hike in the ratio of adsorption sites to oil declined the total adsorption capacity. However, adsorption capacity q_t is measured by dividing the adsorbed oil amount by the amount of the adsorbent, and the increase in the amount of adsorbed

oil is lower than the increase in the amount of adsorbent, leading to a decreasing trend in the adsorption capacity. The effect of adsorbent dosage on the removal efficiency and the adsorption capacity was compared for pristine, pre-treated, and PMMA-g-WS by varying the adsorbent dosage from 5 mg to 15 mg while keeping the oil concentration constant at 300 ppm. The order of oil removal efficiency with respect to the increase in dosage is PMMA-g-WS > pre-treated WS > pristine WS (Figure 2.6 c and d). This reflects the highest adsorptive oil separation efficiency of the PMMA-g-WS as the surface modification enabled easy penetration of oil by exposing the macropores as evident from the BET results and SEM micrographs. More importantly, it significantly increased the hydrophobicity of the surface, which is clearly indicated by the FTIR results.

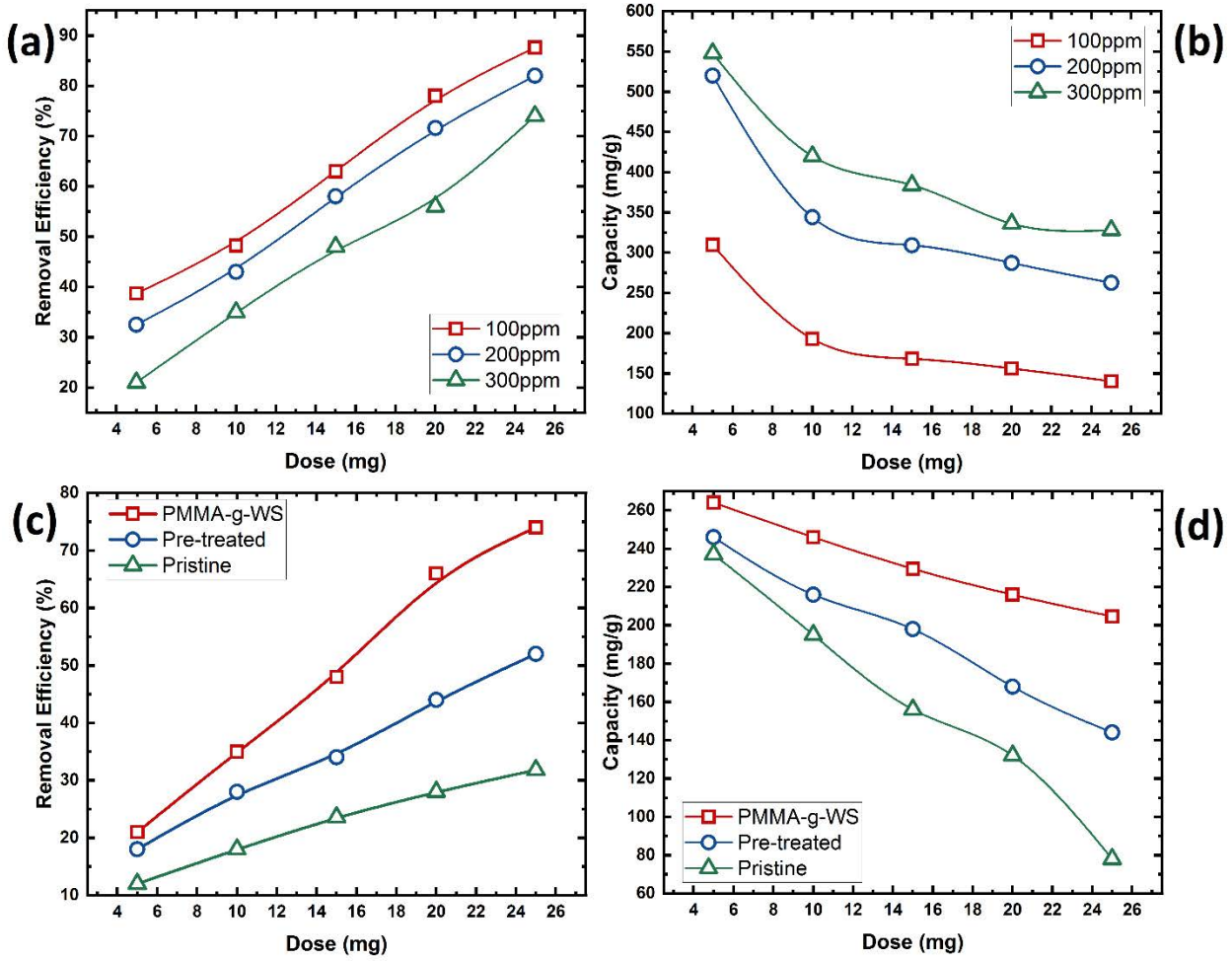

Figure 2.7 Effect of initial oil concentration and adsorbent dosage on the oil removal efficiency (a), and oil adsorption capacity (b) of PMMA-g-WS. Effect of adsorbent dosage on oil removal efficiency (c), and oil adsorption capacity (d) of pristine, pre-treated, and PMMA-g-WS.

2.3.5 Adsorption isotherm models

After evaluating the influence of adsorbent dosage and oil concentration on the oil removal efficiency and adsorption capacity, Langmuir and Freundlich adsorption isotherms were used to understand the oil adsorption mechanism. Figure 2.8 a and b show the linearized plots for Langmuir and Freundlich isotherms, respectively. The Freundlich isotherm provided a better fit to the experimental C_e and q_e values. This strongly indicates the heterogeneity of adsorption sites as well as the involvement of multilayer adsorption of the oil process. Therefore, adsorption efficiency will be higher at the initial stages of adsorption since it is be based on the direct interaction of the adsorption sites with the oil. The adsorption efficiency will be reduced exponentially with the course of time since the adsorption at these stages involves the interaction of the adsorbed oil layer with excess oil in the bulk solution. Diesel oil consisting of different chain lengths of linear hydrocarbons contributed to the multilayer heterogeneous adsorption over the mesoporous structure of PMMA-g-WS [86]. The Freundlich parameters n and K_f values being greater than 1, as shown in Table 1, strongly suggest a higher adsorption capacity of PMMA-g-WS for diesel oil.

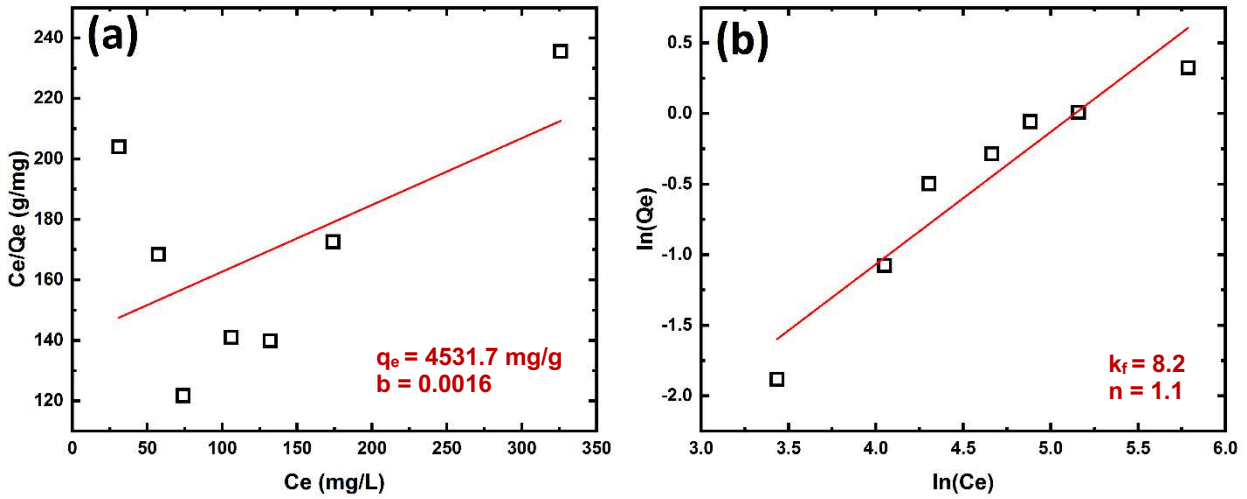

Figure 2.8 Langmuir (a) and Freundlich (b) linear fitting for adsorption of emulsified oil on PMMA-g-WS.

2.3.6 Adsorption kinetics

Large scale application of any adsorption-based filtration system demands the evaluation of the rate of adsorption and the corresponding adsorption equilibrium time. Pseudo-first order and pseudo-second-order kinetics models are widely applied to determine the adsorption kinetics. As seen in Figure 2.9 b, the pseudo-second-order equation provided a better fit with the experimental oil adsorption data for all three WS samples featuring an R^2 value as high as 0.999. The response variable q_e is very close to the experimental values, as mentioned in Table 2.2. The predicted values of q_e from the pseudo-first-order equation, on the other hand, were not even close to the experimental data, even though the R^2 values are reasonably acceptable. Based on these observations, it can be concluded that the adsorption process follows a pseudo-second-order rate for all three WS samples. The pseudo-second-order rate implies that the rate of adsorption decreased with time. This is also consistent with the better fitting of the adsorption data with Freundlich adsorption isotherm, which generally demonstrates higher initial adsorption due to direct interaction of adsorbent with adsorbate followed by slower adsorption in time due to secondary interaction of the surface adsorbed adsorbate with the adsorbate in bulk. The higher surface potential and the corresponding Van der Waals or London dispersion forces between the PMMA grafted on WS and oil molecules contribute to the stronger physisorption and significantly improve the oil uptake rate by this PMMA-g-WS sample.

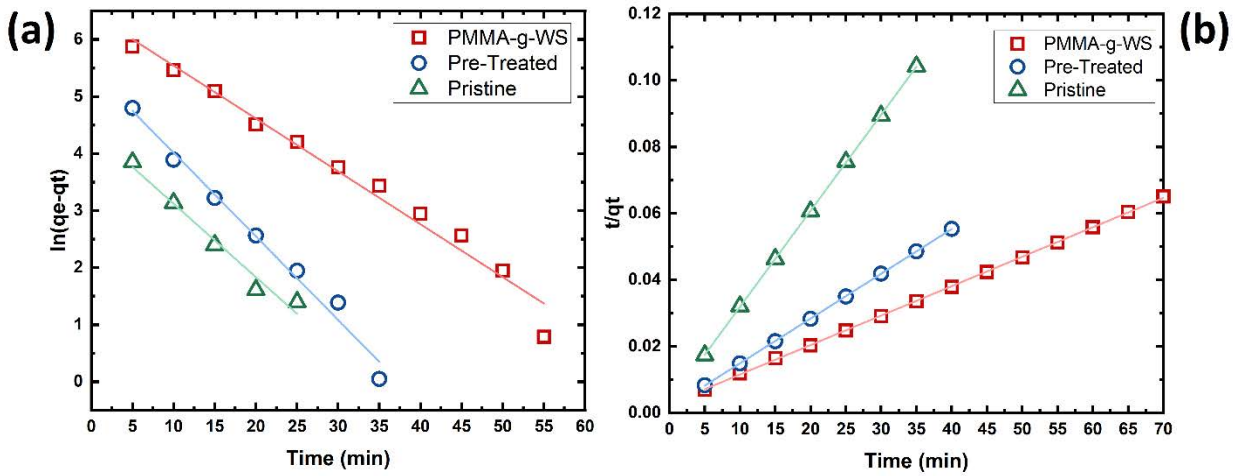

Figure 2.9 Pseudo-first order (a) and pseudo-second-order (b) kinetic models for removal of emulsified oil using pristine, pre-treated, and PMMA-g-WS at ambient temperature and shaking speed of 160 oscillations/min.

Table 2.2: Pseudo-first order and pseudo-second-order kinetic model parameters for removal of emulsified oil using pristine and pre-treated WS as well as PMMA-g-WS.

Sample	Pseudo-first order kinetic parameters			Pseudo-second order kinetic parameters		
	q_e (mg/g)	k_1 (g/mg.h)	R^2	k_2 (g/mg.h)	q_e (mg/g)	R^2
PMMA-g-WS	645	0.0927	0.921	0.0003	1129	0.999
Pre-treated	241	0.1467	0.924	0.0013	741	0.999
Pristine	82	0.1287	0.990	0.0028	346	0.999

2.4 Conclusions

In this study, a simple radical polymerization was explored to enhance the oil adsoptivity of an abundant agricultural by-product wheat straw (WS). An attempt has been made to utilize it as an economical and eco-friendly adsorbent for the separation of oil from oil-in-water emulsions. The pristine WS was pre-treated with alkaline hydrogen peroxide, and PMMA was grafted subsequently in an aqueous solvent using cerium ammonium nitrate as a redox radical initiator. The alkaline hydrogen peroxide pre-treatment played a crucial role in exposing the mesopores, which are vital for any adsorption process. The SEM micrographs, as well as the BET surface results with type 1 H2 (a) hysteresis loops, also indicated clearly the presence of mesopores. The PMMA grafting complemented this by providing the surface hydrophobicity, which is equally essential for the enhancement of hydrophobic-hydrophobic interactions between oil droplets and the grafted surface moieties. The enhanced surface area and the hydrophobicity of PMMA-g-WS resulted in its high oil adhesion property as observed by the 0º oil contact angle, which in turn lead to incremented the oil adsorption by 3.3 times. The experimental adsorptivity data fitted well with Freundlich isotherm, indicating the heterogeneity of adsorption sites as well as multilayer adsorption of oil. The adsorption kinetics was best represented by the pseudo-second-order kinetic model supporting the Freundlich isotherm model of multilayer formation. The adsorption capacity of PMMA-g-WS was found to be 1100 mg/g, which is reasonably high and demonstrates its potential for economical treatment of oily wastewater since the overall cost-efficiency of waste WS along with a simple chemical modification for grafting PMMA process will allow the use of large amount of this adsorbent for large scale applications.

Chapter 3: Integration of poly(methyl methacrylate) grafted adsorption and polyamide-imide microfiltration membranes for separation of oil and water

3.1 Introduction

Industries are significant water consumers and consequently generate huge volumes of wastewater. Numerous industries such as oil refinery, food industry, tannery, meat manufacturing industry, etc. generate toxic hydrocarbon containing effluents [95]. Most of these effluents contain oil in the form of emulsions with droplet size ≤20 μm that are highly stable and hence inhibits the formation of distinct layers of oil and water [1]. Therefore, complete separation of oil and water from emulsified effluents by conventional methods alone such as gravity separation [96], adsorption [22], dissolved air flotation [66]. Membrane filtration, especially the microfiltration and ultrafiltration membranes, is acknowledged as one of the most efficient advanced treatment techniques to separate emulsified oil. High removal efficiency for oil, small footprint, low chemical requirement, and consistent effluent quality are some of the major advantages of this system [11,97,98]. However, conventional polymer membranes are highly prone to fouling either due to adhesion of oil droplets on the surface or pore plugging [12], resulting in the requirement of higher transmembrane pressures. This calls for preliminary treatment of oil-water emulsion to eliminate the free oil with droplet sizes ≥150 μm and dispersed oil contents (20-150 μm) before feeding it to the membrane filtration system. Integration of activated carbon and bentonite adsorption system with PES nano-silica membranes were found to increase the flux significantly by 26.4-30.6% along with providing high rejection of 72% and 90% for TDS and salinity, respectively [15]. In another work [16], precipitative softening and walnut shell filtration as pre-treatment for membrane distillation displayed exceptional efficiencies (≥95%) in eliminating volatile and toxic components such as BTEX (benzene, toluene, ethylbenzene, xylene) from produced water. Numerous other works reported the improvement in performance, in terms of flux and rejection and, more importantly, the membrane lifespan by having a pre-treatment before membrane filtration [7,13,14]. Adsorption is one of the simple, effective, and sustainable technologies available to be applied as a pre-treatment system for separating free and dispersed oil oily wastewaters [17,86]. Wheat straw is an agricultural by-product that is easily available for low

cost, as Canada is one of the top five producers of wheat in the world and produces around 20 MT of wheat per year. It is a porous material that is highly suitable to be used as an adsorbent for oil with abundant hydroxyl groups on the surface. The hydroxyl groups attached to cellulose, hemicellulose, and lignin on the surface of the straw makes it hygroscopic. Therefore, the practical application of this material requires chemical modification to incorporate hydrophobicity [27]. In this study, poly(methyl methacrylate) grafted wheat straw in a fixed bed adsorption system was implemented as a pre-treatment system for oil-water emulsions. In order to overcome the drawbacks of conventional polymer membranes as mentioned earlier, poly(methyl methacrylate) grafted wheat straw in a fixed bed adsorption system was implemented as a pre-treatment system for oil-water emulsions. The effluent of the pre-treatment process was fed to a microfiltration process. Two types of polymeric MF membranes were chosen, namely PES and PAI. In the case of PAI, the amide and imide functionalities incorporate exceptionally high hydrophilicity along with high mechanical, thermal and chemical resistivity. As it also highly important to understand the performance of widely conventional polyethersulfone (PES) microfiltration membranes in treating oil emulsion pre-treated by adsorption, we also performed a comparison study of PAI and PES membranes by conducting systematic cyclic tests for different oil concentrations.

3.2 Experimental

3.2.1 Chemicals

PAI (Torlon® 4000T-HV) was procured from Solvay Advanced Polymers, and PVP polymer additive (reagent grade, MW = 10 kDa) was procured from Sigma Aldrich. Dimethylacetamide (>99%) was obtained from Fischer Scientific.

The details on the materials, methods, and characterizations performed on the PMMA-g-WS and oil emulsion using diesel oil are mentioned in chapter 2 (sections 2.2.1, 2.2.2, 2.2.3, and 2.2.4).

3.2.2 Membrane fabrication

The non-solvent induced phase separation (NIPS) technique was used to fabricate the PAI membranes. A mixture of 8 wt% PAI, 90 wt% DMAc and 2 wt% PVP was stirred at 40ºC for 24 h at 90 rpm. Following the polymer-additive mixture was rested for 24 h at room temperature to eliminate the air bubbles. The polymer solution was then cast on a piece of non-woven fabric with

the aid of an automatic film applicator (TQC, Gardco). The gap height between the applicator and the base plate was fixed to 200 µm, and the casting speed was maintained to be 5 mm/s. Later, the cast films were immersed in a coagulation bath with demineralized water. This brought about the diffusion of DMAc from the polymer solution into the water and helped the formation of a solidified porous membrane. The synthesized membranes were left in the coagulation bath for 2 h to ensure complete leaching of the solvent out of the polymer matrix. The membrane was stored by soaking in demineralized water until testing.

3.3 Membrane characterization

3.3.1 Wettability

The underwater oil contact angle measurements were done using the captive bubble technique. A glass slide with pieces of membranes attached to its surface was submerged in an optically sensitive quartz cuvette filled with demineralized water. 3 µl diesel oil emulsion was placed on the membrane surface to record the contact angle.

3.3.2 Porosity

Porosity ε of the membrane was evaluated using the gravimetric method [35].

$$\varepsilon = \frac{m_1 - m_2}{\rho_{water}} \Big/ \left(\frac{m_1 - m_2}{\rho_{water}} + \frac{m_2}{\rho_{PAI}} \right) \qquad (3.1)$$

where, m_1 and m_2 are the mass of wet and dry membranes respectively, ρ_{water} is the density of water, and ρ_{PAI} is the density of PAI at ambient temperature.

3.3.4 Hydraulic permeability

The hydraulic permeability test was conducted using a dead-end filtration cell with a stirrer (Amicon, UFSC40001). The capacity of the cell is 400 ml, with an effective membrane area of 41.8 cm^2. A pressurized nitrogen gas line was connected to the top part of the cell, and the permeate was collected into a beaker placed on a digital weighing balance (ME4002, Mettler Toledo, USA). The balance was connected to a computer to record the weight of the permeate in a 30s interval. The pure water flux (PWF) was calculated as below:

$$J_w = \frac{\Delta Q}{A\rho\Delta t} \qquad (3.2)$$

where, J_w is pure water permeation flux ($Lm^{-2}h^{-1}$), ΔQ is the permeate volume (L), ρ is the density of the permeate at room temperature, A is the effective membrane area (m^2), and Δt is sampling time (h).

3.3.5 Oil and water separation test

The oil separation efficiency and oil fouling tendency of the PAI membrane, as well as PES membranes, were determined using the dead-end cell with constant stirring. The membranes were first compacted at 3 psi to reach a steady PWF, and the PWF (J_{wo}) was measured. The permeate flux (J_w) was measured for oil emulsions of concentrations 100, 200, 300, and 500 ppm followed by the splashing of the membrane for around 20s with distilled water. The PWF was recorded again prior to permeate flux during the second cycle after regeneration (J_{w1}), in order to understand the fouling tendency of the membranes. The flux decline (FD), flux recovery ratio (FRR), and percentage of oil rejection (R) was calculated using the below equations.

$$FD = \left(1 - \frac{J_w}{J_{w0}}\right) X100 \qquad (3.3)$$

$$FRR = \frac{J_{w1}}{J_{wo}} X100 \qquad (3.4)$$

$$R = \left[1 - \frac{C_{OP}}{C_{OF}}\right] X100 \qquad (3.5)$$

where, C_{OF} and C_{OP} are the concentrations of oil in feed and permeate, respectively.

3.3.6 Oil emulsion characterization

The details of the preparation and characterization of oil emulsion have been mentioned in detail in chapter 2 (sections 2.2.5 and 2.2.6).

3.3.7 Integrated adsorption and membrane filtration system

Continuous study of oil adsorption is extremely important to understand the breakthrough behavior and hence the feasibility of using the PMMA-g-WS for large scale applications. A polyvinyl

chloride (PVC) column of 2.5 cm diameter and 15 cm length was used to perform the breakthrough behavior of oil adsorption on PMMA-g-WS. The PMMA-g-WS bed of height 2 cm was fixed firmly using glass wool. The remaining space of the column, both above and below, was filled with 4 mm glass beads to ensure uniform flow of emulsion and to avoid channeling of flow. A peristaltic pump (Shenchen LabV6) was used to pump the emulsion at a flow rate of 3 ml/min in up-flow mode. The emulsion was continuously stirred throughout the process. The emulsion was fed into the column continuously until there was a breakthrough, and the column reached exhaustion point where the concentration of emulsion at the outlet was the same as the inlet. The adsorbent was then regenerated by passing ethanol at 3ml/min in downflow mode and left for 24 h before conducting the next cycle [86]. The subsequent cycle of adsorption was then conducted to analyze the breakthrough behavior of the column after regeneration and reusability of the PMMA-g-WS. The amount of oil adsorbed by the column q_{total} in mg, $_{the}$ amount of oil delivered to the column m_{total} in mg, and total removal percentage of oil were determined using the following equations [99].

$$q_{total} = \frac{Q}{1000}\int_0^{t_{total}} C_{ad}.\,dt \tag{3.6}$$

where, Q is the oil emulsion flow rate in ml/min, C_{ad} is the adsorbed oil concentration in mg/l which is the difference of inlet and outlet oil concentrations, t_{total} is the total flow time in min.

$$m_{total} = \frac{C_o Q t_{total}}{1000} \tag{3.7}$$

where, C_o is the concentration of oil emulsion at column inlet.

$$Total\ oil\ removal(\%) = \frac{q_{total}}{m_{total}} X100 \tag{3.8}$$

The emulsion at the outlet of the column was fed to the dead-end cell, as shown in Figure 3.1.

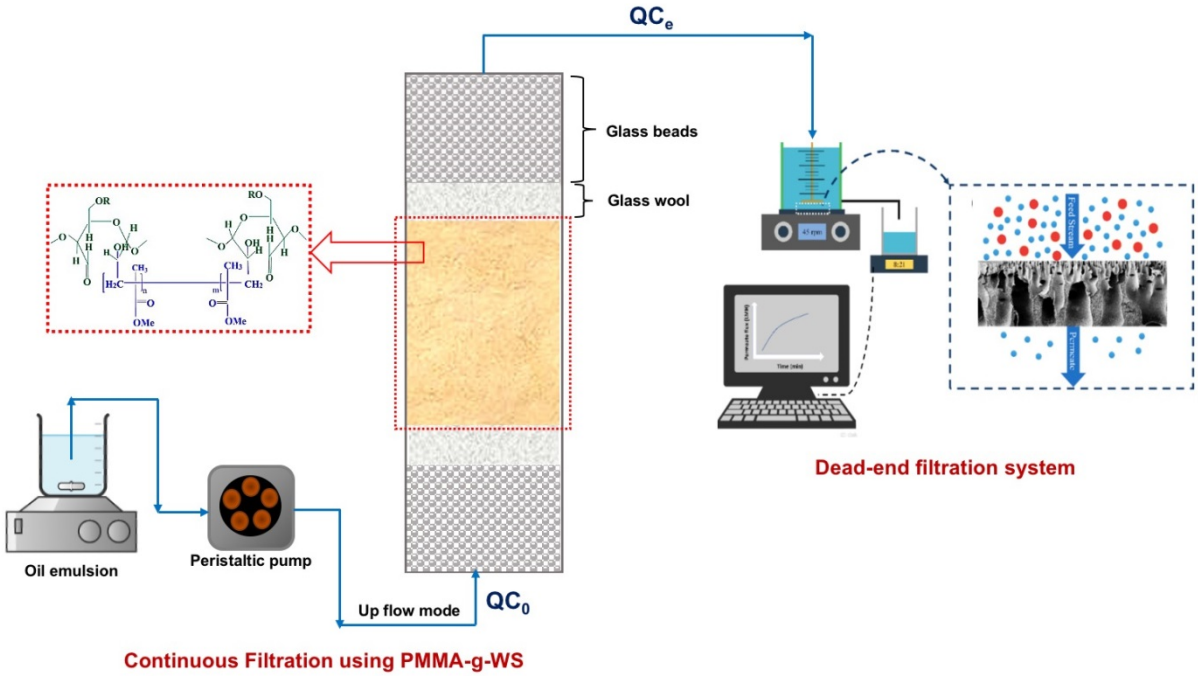

Figure 3.1 Integrated PMMA-g-WS adsorption and PAI/PES microfiltration system for separation of oil and water.

3.4 Results and discussions

3.4.1 Underwater oil wettability and permeation properties of PAI membrane

The underwater oil contact angle measurements for the superoleophobic PAI membranes confirmed that the membranes are superoleophobic. The attachment of the oil droplet onto the membrane surface was very poor, and the oil droplet was drastically repelled by the surface (Figure 3.2). The physicochemical interactions between the membrane surface and the oil droplet is critical for the deposition of oil on the surface of the membrane [35]. The complete repulsion of an oil droplet, in this case, is believed due to the presence of a large number of electron donor components than electron acceptor components on the surface of PAI. This also indicates that the total free energy of cohesion is significantly more than zero, and as a result, the membrane is superhydrophilic and extremely intolerant to the adhesion of oil [35]. The porosity (ε), average pore size (r_p) for the fabricated PAI membrane, was found to be 80% and 179.6 nm, respectively.

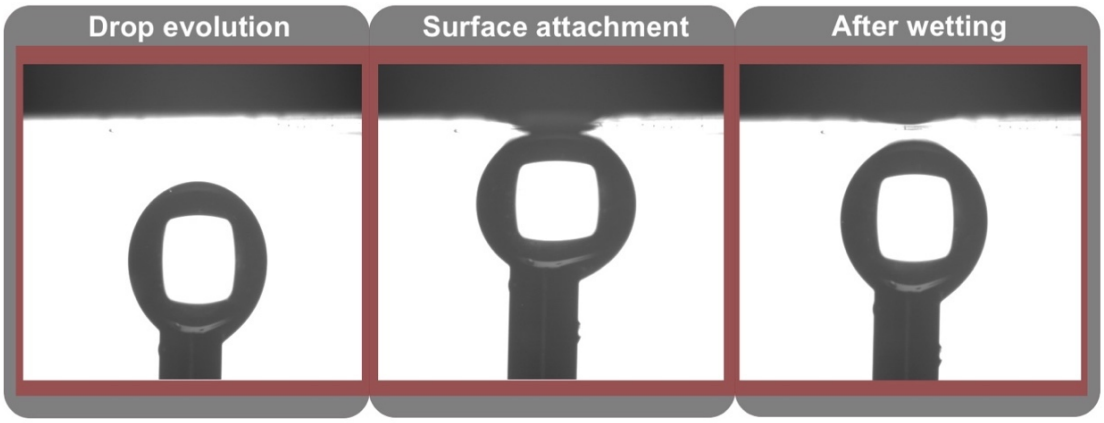

Figure 3.2 Digital images of oil droplets underwater over the fabricated PAI membrane.

3.4.2 Pre-treatment of oil emulsion

The performance of the continuous fixed-bed column with PMMA-g-WS was determined by plotting the ratio of effluent oil concentration to inlet oil concentration (C_t/C_o) versus time, as shown in Figure 3.3. Initial oil concentration is a major limiting factor for the adsorption process. A flow rate of 3 ml/min and was used to feed the oil emulsion in up-flow mode to increase the contact time available for the oil droplet to diffuse from the mesopores on the surface to micropores on the inner walls of the PMMA-g-WS. The equilibrium uptake of oil m_{total} was observed to increase with the increase in initial oil concentration, as shown in Table 3.1, and the unadsorbed oil concentration also increased simultaneously. The C_t/C_o ratio remained close during the initial few minutes as a result of higher hydrophobic interactions with oil droplets and the surface of PMMA-g-WS and availability of sufficient sites for adsorption. However, the ratio was observed to increase rapidly after some time as a result of the progression of saturation of adsorption sites and decreased hydrophobic interactions [86]. Once the column reached the exhaustion point, the C_t/C_o started approaching unity and became constant. This resulted in a decrease in the area above the breakthrough curve, indicating a decrease in the adsorption capacity as well as the total removal efficiency for oil (Table 3.1). The subsequent cycle of adsorption after regeneration with ethanol demonstrated that the column remained highly efficient even after the desorption of oil from the pores of the adsorbent surface. The removal efficiency for 100 ppm initial oil concentration decreased from 52% to 34% during the second cycle, which indicates that the column is suitable for prolonged usage with little decrease in removal efficiency.

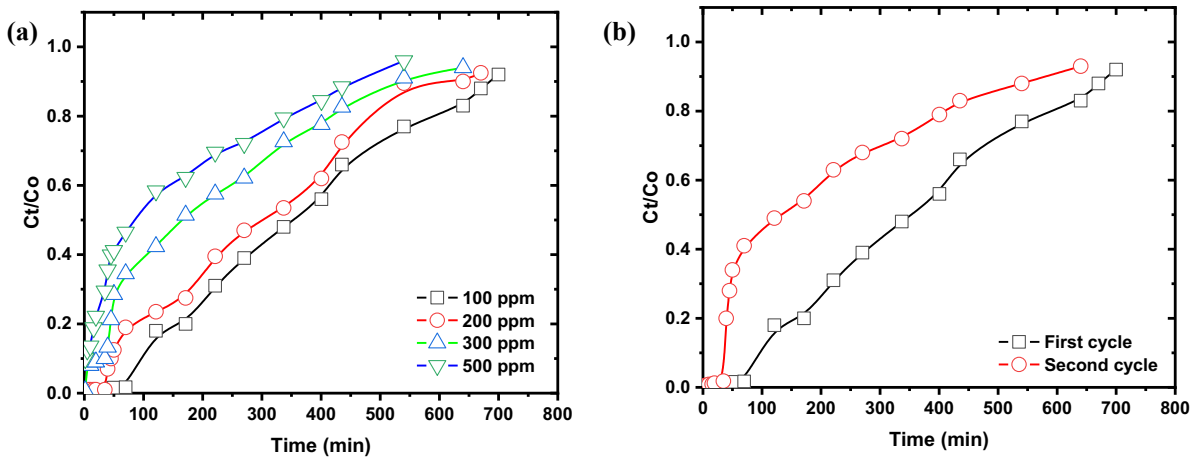

Figure 3.3 Column breakthrough curves of PMMA-g-WS for different oil concentrations of the feed (a), Performance of the column after regeneration for 100 ppm oil concentration (b).

Table 3.1 Fixed bed column parameters for different oil concentrations and regenerated cycle for 100 ppm oil concentration

Initial oil conc. C_o (mg/L)	**Total absorbed oil, q_{total}, (mg)**	**Total oil delivered to the column, m_{total}, (mg)**	**Total removal, (%)**
100 (First cycle)	109	210	52
100 (Second cycle)	64	192	34
200	187	387	46
300	201	576	39
500	245	810	30

3.4.3 Integrated adsorption and membrane filtration

The water flux regeneration capability and fouling resistance of the fabricated PAI membranes as well as the commercial PES membranes were analyzed for oil emulsions with and without the pre-treatment process. The experiments were carried out at similar operating conditions and similar characteristics of the oil emulsion to have a fair correlation of the performance of the membranes with their physicochemical properties such as surface energy, roughness, internal morphology, pore size, and porosity [100]. The oil rejection experiments were conducted for two consecutive cycles at 3 psi pressure for different feed solutions with pre-treatment and without pre-treatment. The normalized permeation flux with initial PWF has been plotted against operating time, as shown in Figures 3.4-3.7.

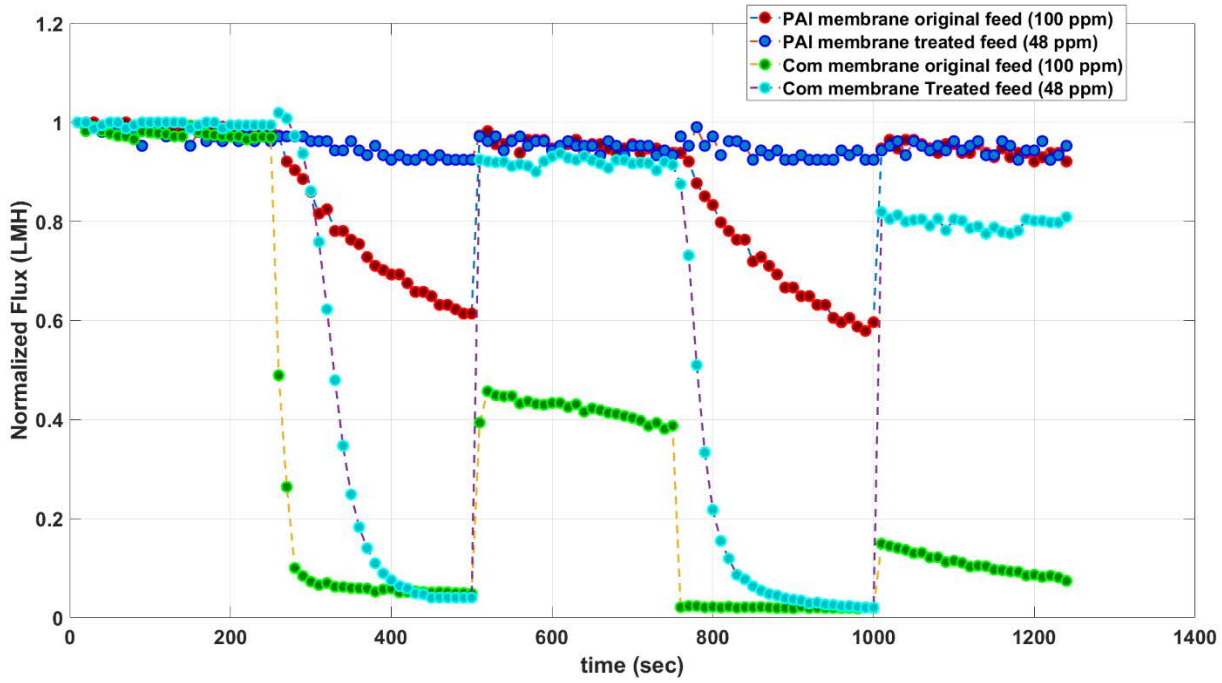

Figure 3.4 Variation of normalized flux (J_w/J_o) of PAI and commercial PES membranes for a pre-treated and original feed of 100 ppm concentration.

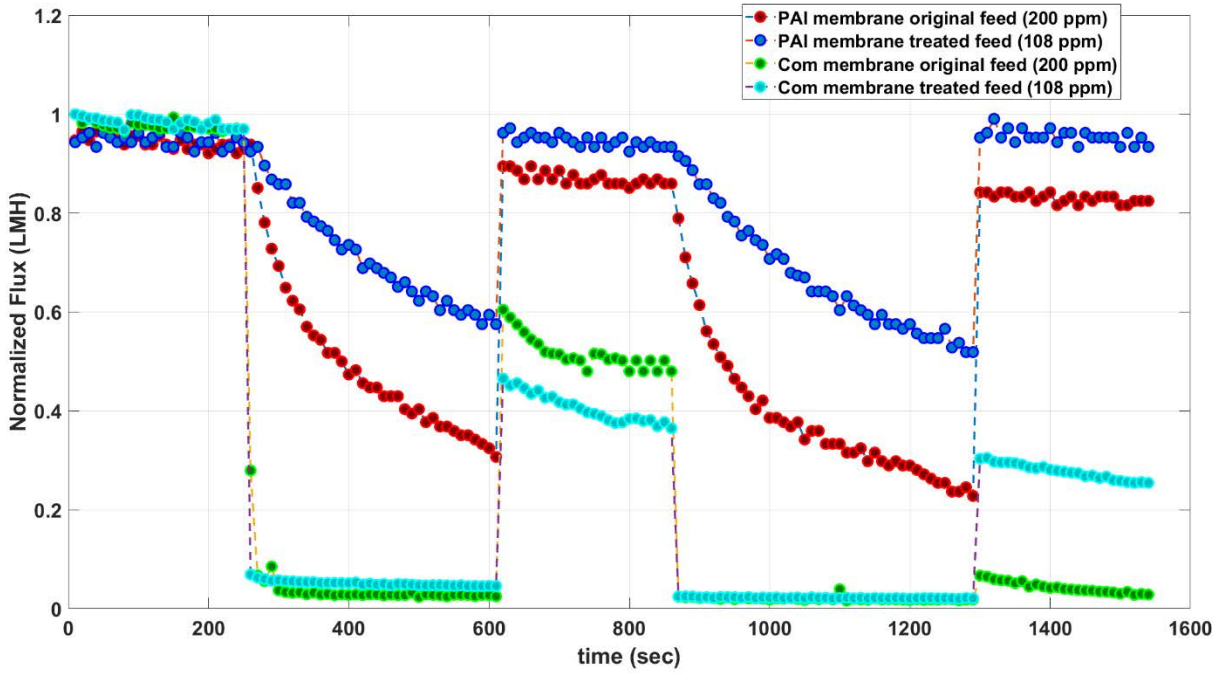

Figure 3.5 Variation of normalized flux (J_w/J_o) of PAI and commercial PES membranes for a pre-treated and original feed of 200 ppm concentration.

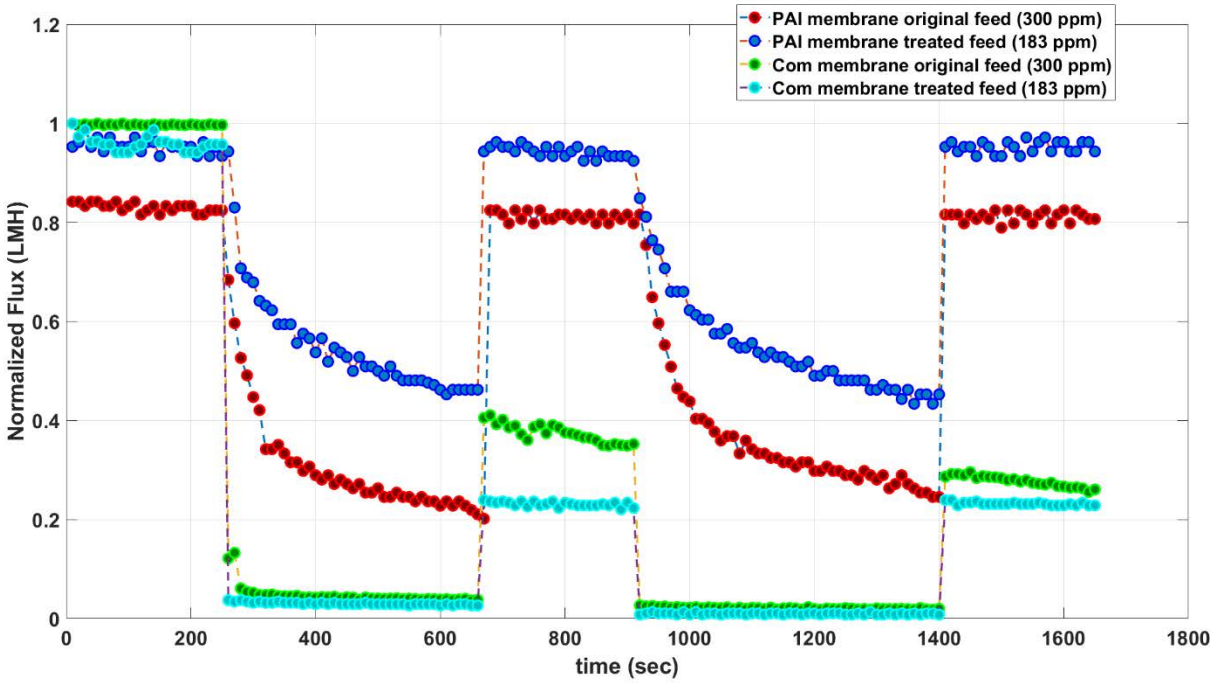

Figure 3.6 Variation of normalized flux (J_w/J_o) of PAI and commercial PES membranes for a pre-treated and original feed of 300 ppm concentration.

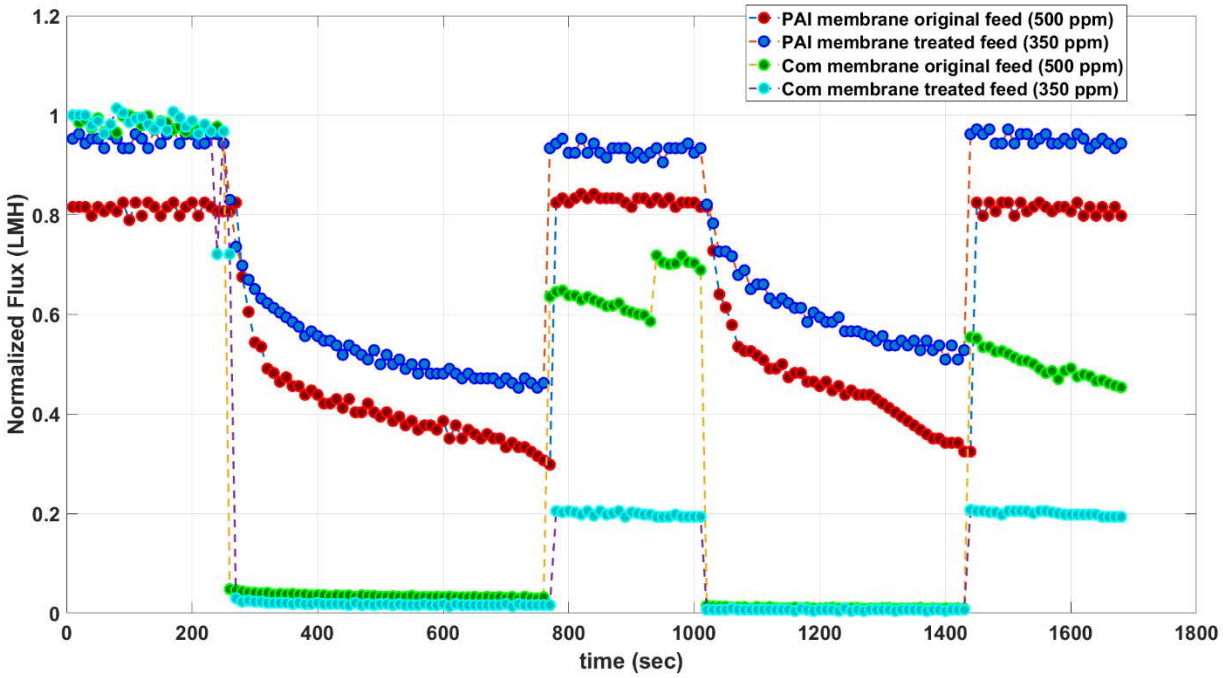

Figure 3.7 Variation of normalized flux (J_w/J_o) of PAI and commercial PES membranes for a pre-treated and original feed of 500 ppm concentration.

The flux decline for the commercial PES membrane was significant compared to the fabricated PAI membrane, as shown in Figure 3.8(a). The FD for commercial membrane for both the cases of with and without pre-treatment by PMMA-g-WS adsorption was almost 100%. This can be attributed to the high fouling tendency for oil irrespective of the concentration. A contrasting observation was made with respect to the PAI membranes. The FD, in this case, was extremely low, especially for the pre-treated feed of all concentrations. The flux decline for a pre-treated feed of concentration 48 ppm was as low as 4%. The FD for PAI was highly dependent on feed concentration. For 48 ppm, the FD was around 4%, and for 500 ppm, it was found to be around 80%. The FRR for the PAI was extremely high for all the cases of pre-treated as well as original feed (Figure 3.8(b)). This demonstrated the excellent resistance to fouling and high stability of the PAI membrane. The FRR was as high as 95% for both original and pre-treated feed of 100 ppm. The pre-treatment by PMMA-g-WS increased the FRR from 84% to 95% in the case of 200, 300, and 500 ppm oil concentrations. The high FRR values for pre-treated feed hence indicate that the pre-treatment has high potential in prolonging membrane lifespan. The exceptionally high flux decline and poor FRR of the commercial PES membrane can be attributed to the cake formation or pore blocking as a result of the hydrophobic nature of PES. This, in turn, is believed to have caused pore-blocking with oil droplets resulting in the formation of concentration polarization and formation of oil film on the surface, causing a decline in water transport. The reason behind the outstanding performance of the PAI membrane can be ascribed to the extremely high underwater oleophobicity (OCA>150°), smoother surfaces, and small average pore size (176.9 nm) [35]. The high flux recovery ratios in the case of the pre-treated feed for both PAI and commercial PES membranes indicate the significance of pre-treatment by PMMA-g-WS. These exciting results show that pre-treatment is highly efficient in increasing the flux and membrane lifespan.

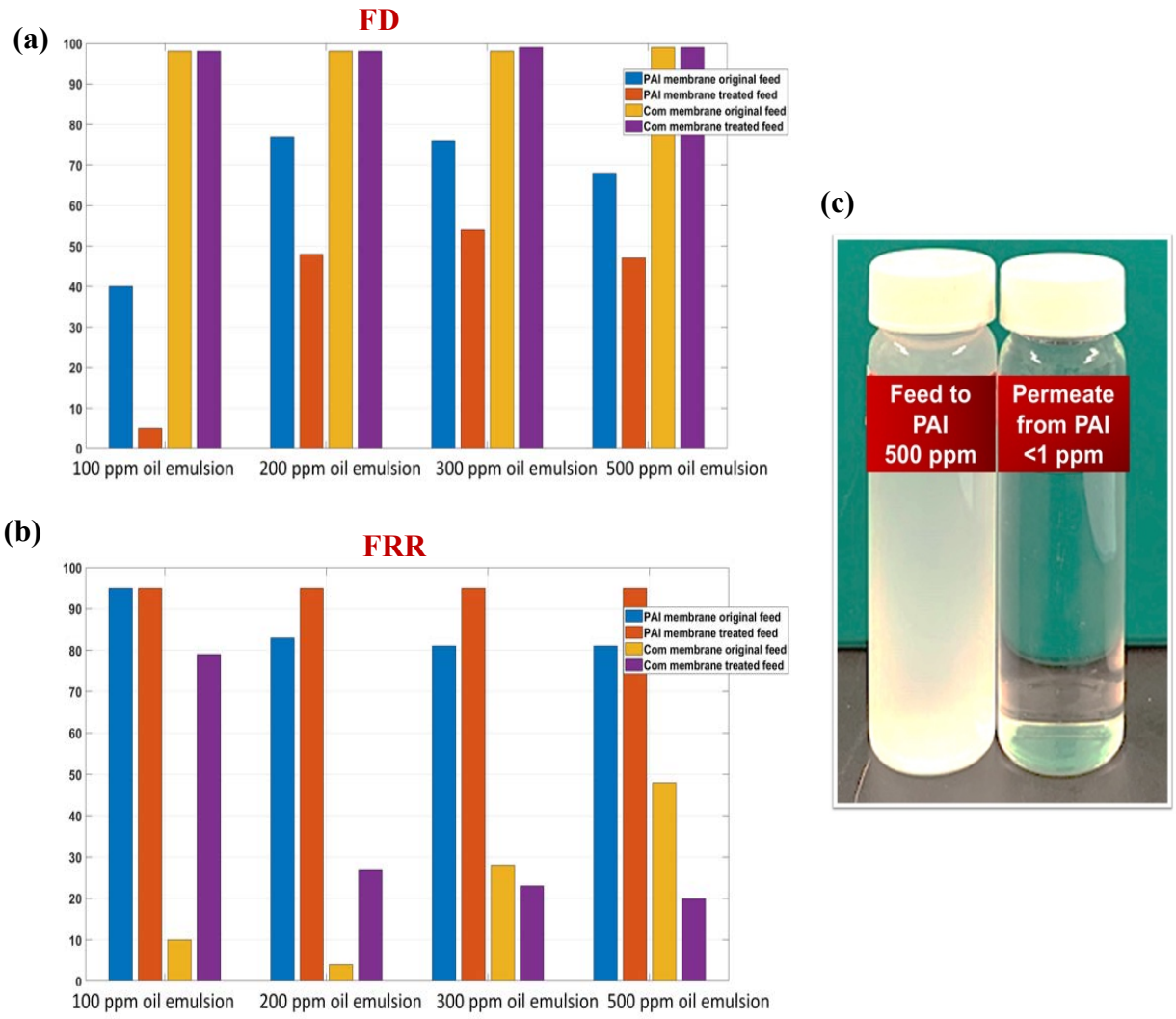

Figure 3.8 Percentage of flux decline (a), Flux recovery ratio for three consecutive cycles (b), Image showing the quality of 500 ppm feed, and its permeate from PAI.

3.5 Conclusion

The effect of pre-treatment of oil-water emulsions on the flux and intensity of fouling for both PAI and commercial PES membranes were studied. The pre-treatment improved the flux significantly for all concentrations of oil in the case of the PAI membrane. The pre-treatment helped in bringing down the flux decline from 40% to 4% in the case of 100 ppm original and pre-treated feed (48 ppm). The commercial PES membranes also exhibited FRR as high as 80% for the pre-treated feed in case of low oil concentrations. Higher oil concentrations, however, caused irreversible fouling of the membrane by pore blocking, as a result of which the FRR was very poor (as low as 3%)

after regeneration. This indicated clearly the poor underwater oleophobicity of the commercial membrane. The fabricated PAI membranes were exceptionally efficient with FRR as high as 95% for 100 ppm, and it declined to 84% for 200, 300, and 500 ppm oil concentrations, respectively, for original feed without pre-treatment. With the pre-treatment, the FRR of 95% could be achieved even for the 200, 300, and 500 ppm feed. Therefore, this study clearly indicates that PMMA-g-WS can be an efficient, cost-effective, and biodegradable adsorbent that can be successfully integrated with membrane filtration to improve the flux and membrane lifespan. The integration of this pre-treatment system, particularly with PAI membranes, serves as an excellent combination to achieve oil removal efficiencies as high as 100%.

Chapter 4: Conclusion and future work

4.1 Conclusion

In this study, an integrated treatment train coupling microfiltration with PAI and commercial polymeric membranes with a fixed bed adsorption system with PMMA grafted wheat straw, an agricultural waste as pre-treatment for efficient treatment of oil-water emulsion, was explored. The study hence provides useful insights into the performance of this unique hybrid system.

A simple radical polymerization was applied to enhance the oil adsoptivity of wheat straw. A chlorine-free alkaline hydrogen peroxide pre-treatment was performed on the pristine straw to ensure (a) exposure of hydroxyl groups of cellulose for grafting PMMA, and (b) easy penetration of oil into the microporous structure of the straw. PMMA was subsequently grafted in an aqueous solvent using cerium ammonium nitrate as a redox radical initiator. The alkaline hydrogen peroxide pre-treatment increased surface sites while the PMMA grafting provided the surface hydrophobicity, which is equally essential for the enhancement of oil adsorption. According to the BET results, the shape of the hysteresis loop for pristine straw correlated with type H2(a) hysteresis according to IUPAC classification and hence indicated the wide distribution of pore cavity compared with the neck distribution. The structure of the tubular vascular interconnected vessels with numerous pits at each node justified this finding. The hysteresis loop shape for pre-treated and PMMA-g-WS, on the other hand, indicated type H2(a), with cavitation. This means that the smaller pore size at a certain critical temperature and adsorption has resulted in desorption through cavitation. Since the pre-treated and PMMA-g-WS were characterized by numerous micropores along with macropores, which was clearly indicated by the SEM micrographs, the narrow tubular micropores might have resulted in cavitation to make way for desorption. The surface area of the samples was in the order pristine>pre-treated>PMMA-g-WS. This trend is mainly believed to be due to the kinetic restrictions associated with the flow of nitrogen into narrowest micropores. A possible explanation is that the interaction of nitrogen with non-polar surface functionalities, like the grafted PMMA in the present work, leads to inaccurate surface area values because such interactions can shift the pore filling pressure of nitrogen to very small relative pressures.

The enhanced surface area and the hydrophobicity of PMMA-g-WS resulted in its high oil adhesion property as observed by the 0 ℃ oil contact angle, which in turn lead to 3.3 times improvement in its oil adsorption capacity compared to pristine WS. The experimental data from the batch study fitted well with Freundlich isotherm, indicating the heterogeneity of adsorption sites as well as multilayer adsorption of oil. The adsorption kinetics was best represented by the pseudo-second order kinetic model supporting the Freundlich isotherm model of multilayer formation. The adsorption capacity of PMMA-g-WS was found to be 1100 mg/g, which is reasonably high and demonstrates its potential for the economical treatment of oily wastewater since the overall cost-efficiency of waste WS and its simpler chemical modification process will allow the use of a large amount of this adsorbent for large scale applications such as for the treatment of oil refinery tailing wastewater and wastewater discharge from petrochemical industries, etc.

The reusability of PMMA-g-WS was analyzed using a bench-scale column setup. The breakthrough curves were obtained for different feed concentrations. The difference in the column exhaustion time was not significant for 100, 200, and 300 ppm feed concentrations. However, the column exhausted swiftly for 500 ppm feed concentration, with oil removal efficiency being 30%. The subsequent cycle after regeneration of the column for 100 ppm oil concentration yielded an oil removal efficiency of 34%. The decrease in the exhaustion time was as low as 50 min. Therefore, the results demonstrate that the high reuse potential of PMMA-g-WS. The availability of the low-cost wheat straw, as well as a simple, cost-effective grafting technique to increase the hydrophobic functional groups on the surface, makes it an excellent candidate to be used as a preliminary treatment system.

The effect of coupling of PMMA-g-WS pre-treatment with PAI and commercial membranes on water flux and fouling tendency was analyzed in the next stage of the study. The pre-treatment improved the flux significantly for all concentrations of oil for the fabricated PAI membrane. The FD for PAI is highly dependent on fee oil concentration. The FD was around 4% for 48 ppm and drastically increased to around 70% for 500 ppm. This indicates the remarkable role of pre-treatment in decreasing the amount of foulants and hence the fouling. In addition, the extremely high flux stability of the PAI membranes especially low feed concentrations can be attributed to

the tremendous underwater oleophobicity, which also a contribution of PVP. It is evident from the contact angle measurements, which displayed strong repulsion of oil droplets from the surface, thereby adding to the total resistivity to fouling and flux decline of the PAI membrane.

The commercial PES membranes also exhibited higher FRR as high as 80% for the pre-treated feed in case of 100 ppm feed concentration. Higher oil concentrations, however, caused irreversible fouling of the commercial membrane by pore blocking, as a result of which the FRR was very low. This indicated clearly the high hydrophobic interactions between the membrane surface and oil droplets. The fabricated PAI membranes were exceptionally efficient with FRR as high as 95% for 100 ppm, and it declined to 84% for 200, 300, and 500 ppm oil concentrations, respectively, for original feed without pre-treatment. With pre-treatment, the FRR as high as 95% could be achieved even for the 200, 300, and 500 ppm feed concentrations. The integration of this pre-treatment system, especially with PAI membranes, serves as an excellent combination to achieve oil removal efficiencies as high as 100%. These results highlight the extremely high potential of utilizing this treatment train to achieve cost and energy-effective treatment of oil-water emulsions in addition to enhancing the membrane lifespan and producing high quality treated water suitable for discharge into water bodies, landscaping, snowmaking, and other beneficial reuse applications.

4.2 Future work

i. In chapter 2, (a) the effect of different concentrations of NaOH and hydrogen peroxide used for pre-treatment of pristine straw using on the porosity and surface area of the straw particles can be explored more, (b) hydrophobic monomers such as styrene can be grafted on cellulose backbone to understanding its effect on hydrophobicity, (c) the oil separation test can be performed for different types of oils with varying viscosity since it significantly influences the permeation and hence the amount of oil adsorbed, (d) application of different mathematical models such as Thomas model, Yoon Nelson model, and Adam Bohart model to the kinetics data is worth exploring to understand other aspects of adsorption, and (e) the surface area and pore distribution should be analyzed with techniques using argon or carbon dioxide instead of nitrogen gas. It is strongly believed

that the interaction of nitrogen with the surface functionalities in the case of PMMA-g-WS, and the kinetic restrictions of the gas to penetrate into narrow micropores in the case of all the three samples might have resulted in the underestimation of the surface area. Wheat straw being plant biomass, is characterized by numerous micropores and ultra-micropores. The accurate estimation of its surface area and pore sizes can open new pathways to utilize it in better ways as an adsorbent.

ii. In chapter 3, (a) the continuous adsorption study using the fixed bed can be performed by varying the flow rate of feed solution and thereby the contact time between the oil droplets and PMMA-g-WS particles, the bed height can also varied to determine its effect on the shape of the breakthrough curve, (b) the performance of the PAI and commercial PES membranes can be checked in crossflow mode, and a comparison with the current results from dead-end mode can be performed, (c) different hydrophilic additives can be added to PAI, and a study on its effect on the underwater oleophobicity can be performed.

References

[1] S. Ibrahim, H.M. Ang, S. Wang, Removal of emulsified food and mineral oils from wastewater using surfactant modified barley straw, Bioresour. Technol. 100 (2009) 5744–5749. doi:10.1016/j.biortech.2009.06.070.

[2] L. Yu, M. Han, F. He, A review of treating oily wastewater, Arab. J. Chem. 10 (2017) S1913–S1922. doi:10.1016/j.arabjc.2013.07.020.

[3] S. Jamaly, A. Giwa, S.W. Hasan, Recent improvements in oily wastewater treatment: Progress, challenges, and future opportunities, J. Environ. Sci. (China). 37 (2015) 15–30. doi:10.1016/j.jes.2015.04.011.

[4] R. Ghidossi, D. Veyret, J.L. Scotto, T. Jalabert, P. Moulin, Ferry oily wastewater treatment, Sep. Purif. Technol. 64 (2009) 296–303. doi:10.1016/j.seppur.2008.10.013.

[5] X.N. Cheng, Y.W. Gong, Treatment of oily wastewater from cold-rolling mill through coagulation and integrated membrane processes, Environ. Eng. Res. 23 (2018) 159–163. doi:10.4491/eer.2016.134.

[6] M.A. Fulazzaky, R. Omar, Removal of oil and grease contamination from stream water using the granular activated carbon block filter, Clean Technol. Environ. Policy. 14 (2012) 965–971. doi:10.1007/s10098-012-0471-8.

[7] Y. Kim, D. Choi, M. Cui, J. Lee, B. Kim, K. Park, H. Jung, B. Lee, Dissolved air flotation separation for pretreatment of membrane bioreactor in domestic wastewater treatment, J. Water Supply Res. Technol. - AQUA. 64 (2015) 186–193. doi:10.2166/aqua.2014.003.

[8] K. Tong, Y. Zhang, G. Liu, Z. Ye, P.K. Chu, Treatment of heavy oil wastewater by a conventional activated sludge process coupled with an immobilized biological filter, Int. Biodeterior. Biodegrad. 84 (2013) 65–71. doi:10.1016/j.ibiod.2013.06.002.

[9] Y. Deng, G. Zhang, R. Bai, S. Shen, X. Zhou, I. Wyman, Fabrication of superhydrophilic and underwater superoleophobic membranes via an in situ crosslinking blend strategy for highly efficient oil/water emulsion separation, J. Memb. Sci. 569 (2019) 60–70. doi:10.1016/j.memsci.2018.09.069.

[10] S. Zarghami, T. Mohammadi, M. Sadrzadeh, B. Van der Bruggen, Superhydrophilic and underwater superoleophobic membranes - A review of synthesis methods, Prog. Polym. Sci. 98 (2019) 101166. doi:10.1016/j.neubiorev.2019.07.019.

[11] and y. Z. T. Yuan, J. Meng, T. Hao, Z. Wang, A scalable method toward superhydrophilic and underwater superoleophobic PVDF membranes for effective oil/water emulsion separation, (n.d.).

[12] anie.201308183 (1).pdf, (n.d.).

[13] C. Akarsu, Y. Ozay, N. Dizge, H.E. Gulsen, H. Ates, B. Gozmen, M. Turabik, Electrocoagulation and nanofiltration integrated process application in purification of bilge water using response surface methodology, Water Sci. Technol. 74 (2016) 564–579. doi:10.2166/wst.2016.168.

[14] Y. Rasouli, M. Abbasi, S.A. Hashemifard, Oily wastewater treatment by adsorption-membrane filtration hybrid process using powdered activated carbon, natural zeolite powder and low cost ceramic membranes, Water Sci. Technol. 76 (2017) 895–908. doi:10.2166/wst.2017.247.

[15] T.D. Kusworo, N. Aryanti, Qudratun, D.P. Utomo, Oilfield produced water treatment to clean water using integrated activated carbon-bentonite adsorbent and double stages membrane process, Chem. Eng. J. 347 (2018) 462–471. doi:10.1016/j.cej.2018.04.136.

[16] Z. Zhang, X. Du, K.H. Carlson, C.A. Robbins, T. Tong, Effective treatment of shale oil and gas produced water by membrane distillation coupled with precipitative softening and walnut shell filtration, Desalination. 454 (2019) 82–90. doi:10.1016/j.desal.2018.12.011.

[17] Q.L. Zhao, E.H. Liu, G.X. Wang, Z.H. Hou, X.H. Zhan, L.C. Liu, H. Wu, Photoinduced ICAR ATRP of methyl methacrylate with AIBN as photoinitiator, J. Polym. Res. 21 (2014). doi:10.1007/s10965-014-0444-1.

[18] A.L.P. Xavier, O.F.H. Adarme, L.M. Furtado, G.M.D. Ferreira, L.H.M. da Silva, L.F. Gil, L.V.A. Gurgel, Modeling adsorption of copper(II), cobalt(II) and nickel(II) metal ions from aqueous solution onto a new carboxylated sugarcane bagasse. Part II: Optimization of monocomponent fixed-bed column adsorption, J. Colloid Interface Sci. 516 (2018) 431–445. doi:10.1016/j.jcis.2018.01.068.

[19] G.W. Beall, The use of organo-clays in water treatment, Appl. Clay Sci. 24 (2003) 11–20. doi:10.1016/j.clay.2003.07.006.

[20] Y. Xu, H. Yang, D. Zang, Y. Zhou, F. Liu, X. Huang, J.S. Chang, C. Wang, S.H. Ho, Preparation of a new superhydrophobic/superoleophilic corn straw fiber used as an oil absorbent for selective absorption of oil from water, Bioresour. Bioprocess. 5 (2018).

doi:10.1186/s40643-018-0194-8.

[21] K.K. Ongarbayev Ã Â•K, Oil Sorption by Heat-Treated Rice Husks, J. Pet. Environ. Biotechnol. 06 (2015) 10–12. doi:10.4172/2157-7463.1000243.

[22] K.Y.A. Lin, S.Y. Chen, Enhanced removal of oil droplets from oil-in-water emulsions using polyethylenimine-modified rice husk, Waste and Biomass Valorization. 6 (2015) 495–505. doi:10.1007/s12649-015-9384-1.

[23] G. Deschamps, H. Caruel, M.-E. Borredon, C. Bonnin, C. Vignoles, Oil Removal from Water by Selective Sorption on Hydrophobic Cotton Fibers. 1. Study of Sorption Properties and Comparison with Other Cotton Fiber-Based Sorbents, Environ. Sci. Technol. 37 (2003) 1013–1015. doi:10.1021/es020061s.

[24] G. Alaa El-Din, A.A. Amer, G. Malsh, M. Hussein, Study on the use of banana peels for oil spill removal, Alexandria Eng. J. (2017). doi:10.1016/j.aej.2017.05.020.

[25] Y. Xing, G. Wang, Poly(methacrylic acid)-modified sugarcane bagasse for enhanced adsorption of cationic dye, Environ. Technol. 30 (2009) 611–619. doi:10.1080/09593330902838098.

[26] M.O. Adebajo, R.L. Frost, J.T. Kloprogge, O. Carmody, S. Kokot, Porous Materials for Oil Spill Cleanup : A Review of Synthesis, J. Porous Mater. 10 (2003) 159–170. doi:10.1023/A:1027484117065.

[27] X.F. Sun, R. Sun, J.X. Sun, Acetylation of rice straw with or without catalysts and its characterization as a natural sorbent in oil spill cleanup, J. Agric. Food Chem. 50 (2002) 6428–6433. doi:10.1021/jf020392o.

[28] D. Zang, M. Zhang, F. Liu, C. Wang, Superhydrophobic/superoleophilic corn straw fibers as effective oil sorbents for the recovery of spilled oil, J. Chem. Technol. Biotechnol. 91 (2016) 2449–2456. doi:10.1002/jctb.4834.

[29] H. Moazed, T. Viraraghavan, Removal of oil from water by bentonite, Proceedings, Annu. Conf. - Can. Soc. Civ. Eng. 4 (1999) 221–229. doi:10.1061/(ASCE)1090-025X(2005)9.

[30] A. Mukherjee, S. Halder, D. Datta, K. Anupam, B. Hazra, M. Kanti Mandal, G. Halder, Free radical induced grafting of acrylonitrile on pre-treated rice straw for enhancing its durability and flame retardancy, J. Adv. Res. 8 (2017) 73–83. doi:10.1016/j.jare.2016.12.003.

[31] A.S. Singha, R.K. Rana, Microwave induced graft copolymerization of methyl

methacrylate onto Lignocellulosic Fibers, Int. J. Polym. Anal. Charact. 15 (2010) 370–386. doi:10.1080/1023666X.2010.500539.

[32] V.K. Thakur, M.K. Thakur, R.K. Gupta, Graft Copolymers from Natural Polymers Using Free Radical Polymerization, Int. J. Polym. Anal. Charact. 18 (2013) 495–503. doi:10.1080/1023666X.2013.814241.

[33] M. Banerjee, R. kumar Basu, S.K. Das, Adsorptive removal of Cu(II) by pistachio shell: Isotherm study, kinetic modelling and scale-up designing — continuous mode, Environ. Technol. Innov. 15 (2019) 100419. doi:10.1016/j.eti.2019.100419.

[34] B.S. Enoh, C.O. Ogwuche, Graft Copolymerization of Acrylamide and Methylmethacrylate onto Cellulose Fibres: Influence of Initiator in Gel Formation, Int. J. Chem. Technol. 7 (2015) 12–18. doi:10.3923/ijct.2015.12.18.

[35] N. Helali, M. Rastgar, M.F. Ismail, M. Sadrzadeh, Development of underwater superoleophobic polyamide-imide (PAI) microfiltration membranes for oil/water emulsion separation, Sep. Purif. Technol. 238 (2020) 116451.

[36] A. Asad, M. Rastgar, H. Nazaripoor, M. Sadrzadeh, Durability and Recoverability of Soft Lithographically Patterned Hydrogel Molds for the Formation of Phase Separation Membranes, Micromachines. 11 (2020) 108.

[37] A. Asad, D. Sameoto, M. Sadrzadeh, Overview of membrane technology, Elsevier Inc., 2020. doi:10.1016/b978-0-12-816710-6.00001-8.

[38] H. Matsuyama, T. Maki, M. Teramoto, K. Kobayashi, Effect of PVP additive on porous polysulfone membrane formation by immersion precipitation method, Sep. Sci. Technol. 38 (2003) 3449–3458. doi:10.1081/SS-120023408.

[39] L. Yan, Y.S. Li, C.B. Xiang, S. Xianda, Effect of nano-sized Al2O3-particle addition on PVDF ultrafiltration membrane performance, J. Memb. Sci. 276 (2006) 162–167. doi:10.1016/j.jsb.2006.03.024.

[40] Metcalf and Eddy, Wastewater Engineering: Treatment and reuse", Tata Mc. Graw Hill, Fourth edition (2003).

[41] P. Karami, B. Khorshidi, M. Mcgregor, J.T. Peichel, B.P. Soares, M. Sadrzadeh, Thermally stable thin fi lm composite polymeric membranes for water treatment : A review, J. Clean. Prod. 250 (2020) 119447. doi:10.1016/j.jclepro.2019.119447.

[42] S. Veeraraghavan, Modeling adsorption in liquid-solid beds, 44 (1989) 2333–2344.

[43] M. Thommes, K. Kaneko, A. V. Neimark, J.P. Olivier, F. Rodriguez-Reinoso, J. Rouquerol, K.S.W. Sing, Physisorption of gases, with special reference to the evaluation of surface area and pore size distribution (IUPAC Technical Report), Pure Appl. Chem. 87 (2015) 1051–1069. doi:10.1515/pac-2014-1117.

[44] M.A.E. de Franco, C.B. de Carvalho, M.M. Bonetto, R. de Pelegrini Soares, L.A. Féris, Diclofenac removal from water by adsorption using activated carbon in batch mode and fixed-bed column: Isotherms, thermodynamic study and breakthrough curves modeling, J. Clean. Prod. 181 (2018) 145–154. doi:10.1016/j.jclepro.2018.01.138.

[45] A.T. Mohd Din, B.H. Hameed, A.L. Ahmad, Batch adsorption of phenol onto physiochemical-activated coconut shell, J. Hazard. Mater. 161 (2009) 1522–1529. doi:10.1016/j.jhazmat.2008.05.009.

[46] B.H. Hameed, M.I. El-Khaiary, Batch removal of malachite green from aqueous solutions by adsorption on oil palm trunk fibre: Equilibrium isotherms and kinetic studies, J. Hazard. Mater. 154 (2008) 237–244. doi:10.1016/j.jhazmat.2007.10.017.

[47] J. Xu, L. Wang, Y. Zhu, Decontamination of bisphenol A from aqueous solution by graphene adsorption, Langmuir. 28 (2012) 8418–8425. doi:10.1021/la301476p.

[48] M. Banerjee, S. Sain, A. Mukhopadhyay, S. Sengupta, T. Kar, D. Ray, Surface Treatment of Cellulose Fibers with Methylmethacrylate for Enhanced Properties of in situ Polymerized PMMA / Cellulose Composites, 39808 (2014) 1–9. doi:10.1002/app.39808.

[49] V.K. Thakur, M.K. Thakur, R.K. Gupta, Synthesis of lignocellulosic polymer with improved chemical resistance through free radical polymerization, Int. J. Biol. Macromol. 61 (2013) 121–126. doi:10.1016/j.ijbiomac.2013.06.045.

[50] A. Serbezov, Effect of the process parameters on the lenght of the mass transfer zone during product withdrawal in pressure swing adsorption cycles, Chem. Eng. Sci. 56 (2001) 4673–4684. doi:10.1016/S0009-2509(01)00121-X.

[51] Y.S. Al-Degs, M.A.M. Khraisheh, S.J. Allen, M.N. Ahmad, Adsorption characteristics of reactive dyes in columns of activated carbon, J. Hazard. Mater. 165 (2009) 944–949. doi:10.1016/j.jhazmat.2008.10.081.

[52] S. Kundu, S.S. Kavalakatt, A. Pal, S.K. Ghosh, M. Mandal, T. Pal, Removal of arsenic using hardened paste of Portland cement: Batch adsorption and column study, Water Res. 38 (2004) 3780–3790. doi:10.1016/j.watres.2004.06.018.

[53] M. Kapoor, D. Panwar, G.S. Kaira, Bioprocesses for Enzyme Production Using Agro-Industrial Wastes: Technical Challenges and Commercialization Potential, Agro-Industrial Wastes as Feed. Enzym. Prod. Apply Exploit Emerg. Valuab. Use Options Waste Biomass. (2016) 61–93. doi:10.1016/B978-0-12-802392-1.00003-4.

[54] R. Liu, H. Yu, Y. Huang, Structure and morphology of cellulose in wheat straw, Cellulose. 12 (2005) 25–34. doi:10.1007/s10570-004-0955-8.

[55] E. Lv, W. Xia, M. Tang, Y. Pu, Preparation of an Efficient Oil-Spill Adsorbent Based on Wheat Straw, BioResources. 12 (2017) 296–315.

[56] E.M. Rubin, Genomics of cellulosic biofuels, Nature. 454 (2008) 841–845. doi:10.1038/nature07190.

[57] A. Bhattacharya, B.N. Misra, Grafting: a versatile means to modify polymers: Techniques, factors and applications, Prog. Polym. Sci. 29 (2004) 767–814. http://www.sciencedirect.com/science/article/B6TX2-4CY0FJ3-1/2/9301524a43e0e26a7aebd3198cb0d4f0.

[58] A. Beshay, Lignocellulose and Cellulose in the Presence of, (1982) 253–268.

[59] N. Shiraishi, T. Aoki, M. Norimoto, M. Okumura, Thermoplasticization of Cellulose and Wood by Graft Copolymerization and Acylation, (1982) 321–348. doi:10.1021/bk-1982-0187.ch020.

[60] D. J. McDowall, B. S. Gupta and V. Stanett, The ceric ion method of grafting acrylic acid to cellullose, ACS symposium series, American Chemical Society. (1982) 46-55.

[61] K.E. Russell, Free radical graft polymerization and copolymerization at higher temperatures, Prog. Polym. Sci. 27 (2002) 1007–1038. doi:10.1016/S0079-6700(02)00007-2.

[62] M. Chaimbergt, Y. Cohen, Free-radical graft polymerization of vinylpyrrolidone onto silica, Ind. Eng. Chem. Res. 30 (1991) 2534–2542.

[63] B. Ranby and L. Gadda, Graft copolymerization of vinyl monomers onto cellulsic fibers, ACS symposium series, American Chemical Society. (1982) 34-43.

[64] A.H.F. Tahir, N.O. Kariem, S.A. Ibrahim, COD Removal of Edible Oil Content in Wastewater by Advanced Oxidation Process, Environ. Nat. Resour. Res. 6 (2016) 57. doi:10.5539/enrr.v6n2p57.

[65] K. Okiel, M. El-Sayed, M.Y. El-Kady, Treatment of oil–water emulsions by adsorption

onto activated carbon, bentonite and deposited carbon, Egypt. J. Pet. 20 (2011) 9–15. doi:10.1016/j.ejpe.2011.06.002.

[66] M. Hanafy, H.I. Nabih, Treatment of oily wastewater using dissolved air flotation technique, Energy Sources, Part A Recover. Util. Environ. Eff. 29 (2007) 143–159. doi:10.1080/009083190948711.

[67] N. Chawaloesphonsiya, P. Painmanakul, Study of Cutting-Oil Emulsion Separation by Coalescer Process in Terms of Medium Characteristics and Bed Packing, Sep. Sci. Technol. 49 (2014) 2960–2967. doi:10.1080/01496395.2014.943768.

[68] K. Dermentzis, D. Marmanis, A. Christoforidis, K. Ouzounis, Electrochemical reclamation of wastewater resulted from petroleum tanker truck cleaning, Environ. Eng. Manag. J. 13 (2014) 2395–2399.

[69] C. Sun, T. Leiknes, J. Weitzenböck, B. Thorstensen, Development of an integrated shipboard wastewater treatment system using biofilm-MBR, Sep. Purif. Technol. 75 (2010) 22–31. doi:10.1016/j.seppur.2010.07.005.

[70] M. Capodici, A. Cosenza, D. Di Trapani, G. Mannina, M. Torregrossa, G. Viviani, Treatment of oily wastewater with membrane bioreactor systems, Water (Switzerland). 9 (2017). doi:10.3390/w9060412.

[71] Q.F. Alsalhy, R.S. Almukhtar, H.A. Alani, Oil Refinery Wastewater Treatment by Using Membrane Bioreactor (MBR), Arab. J. Sci. Eng. 41 (2016) 2439–2452. doi:10.1007/s13369-015-1881-9.

[72] O.K. Abass, X. Wu, Y. Guo, K. Zhang, Membrane Bioreactor in China: A Critical Review, Int. J. Membr. Sci. Technol. 2 (2015) 29–47. doi:10.15379/2410-1869.2015.02.02.04.

[73] L. Deng, W. Guo, H. Hao, H. Zhang, J. Wang, J. Li, Bioresource Technology Biofouling and control approaches in membrane bioreactors, Bioresour. Technol. 221 (2016) 656–665. doi:10.1016/j.biortech.2016.09.105.

[74] H.H. Sokker, N.M. El-Sawy, M.A. Hassan, B.E. El-Anadouli, Adsorption of crude oil from aqueous solution by hydrogel of chitosan based polyacrylamide prepared by radiation induced graft polymerization, J. Hazard. Mater. 190 (2011) 359–365. doi:10.1016/j.jhazmat.2011.03.055.

[75] A. Zanoletti, I. Vassura, E. Venturini, M. Monai, T. Montini, S. Federici, A. Zacco, L.

Treccani, E. Bontempi, A new porous hybrid material derived from silica fume and alginate for sustainable pollutants reduction, Front. Chem. 6 (2018) 1–13. doi:10.3389/fchem.2018.00060.

[76] I. Ali, A. Arsh, X.Y. Mbianda, A. Burakov, E. Galunin, I. Burakova, E. Mkrtchyan, A. Tkachev, V. Grachev, Graphene based adsorbents for remediation of noxious pollutants from wastewater, Environ. Int. 127 (2019) 160–180. doi:10.1016/j.envint.2019.03.029.

[77] K. Mehmood, Y. Wu, L. Wang, S. Yu, P. Li, X. Chen, Z. Li, Y. Zhang, M. Li, W. Liu, Y. Zhu, D. Rosenfeld, J. Seinfeld, Relative effects of open biomass and crop straw burning on haze formation over central and eastern China: modelling study driven by constrained emissions, Atmos. Chem. Phys. 20 (2020) 1–43. doi:10.5194/acp-2019-808.

[78] X. Xu, B.Y. Gao, X. Tan, Q.Y. Yue, Q.Q. Zhong, Q. Li, Characteristics of amine-crosslinked wheat straw and its adsorption mechanisms for phosphate and chromium (VI) removal from aqueous solution, Carbohydr. Polym. 84 (2011) 1054–1060. doi:10.1016/j.carbpol.2010.12.069.

[79] A. Kezerle, N. Velic, D. Hasenay, D. Kovačevic, Lignocellulosic materials as dye adsorbents: Adsorption of methylene blue and congo red on brewers' spent grain, Croat. Chem. Acta. 91 (2018) 53–64. doi:10.5562/cca3289.

[80] Q. Wang, M. Yu, G. Chen, Q. Chen, J. Tai, Facile Fabrication of Superhydrophobic/Superoleophilic Cotton for Highly Efficient Oil/Water Separation, BioResources. 12 (2016) 643–654. doi:10.15376/biores.12.1.643-654.

[81] bk-1982-0187.ch001.pdf, (n.d.).

[82] B. Tosh, C.R. Routray, Grafting of cellulose based materials : a review, Chem. Sci. Rev. Lett. 3 (2014) 74–92.

[83] M. Via, H. Atrp, Synthesis of cellulose-graft-poly(methyl methacrylate) via homogeneous atrp, 6 (2011) 2941–2953.

[84] A. Fakhru'L-Razi, I.Y.M. Qudsieh, W.M.Z.W.Y.M.B. Ahmad, M.Z.A. Rahman, Graft copolymerization of methyl methacrylate onto sago starch using ceric ammonium nitrate and potassium persulfate as redox initiator systems, J. Appl. Polym. Sci. 82 (2001) 1375–1381. doi:10.1002/app.1974.

[85] B.E. Guettler, C. Moresoli, L.C. Simon, Contact angle and surface energy analysis of soy materials subjected to potassium permanganate and autoclave treatment, Ind. Crops Prod.

50 (2013) 219–226. doi:10.1016/j.indcrop.2013.06.035.

[86] A. Diraki, H. Mackey, G. McKay, A.A. Abdala, Removal of oil from oil–water emulsions using thermally reduced graphene and graphene nanoplatelets, Chem. Eng. Res. Des. 137 (2018) 47–59. doi:10.1016/j.cherd.2018.03.030.

[87] F. A. Ilawi, M. B. Ahmad, N. A. Ibrahim, M. Z. Rahman, K. Z. Dahlan, and W. M. Yunus, optimization condition for grafting reaction of poly(methyl methacrylate) onto rubberwood fiber. Polymer International. 53 (2004) 386-391.

[88] K.A. Cychosz, M. Thommes, Progress in the Physisorption Characterization of Nanoporous Gas Storage Materials, Engineering. 4 (2018) 559–566. doi:10.1016/j.eng.2018.06.001.

[89] P.A. Monson, Understanding adsorption/desorption hysteresis for fluids in mesoporous materials using simple molecular models and classical density functional theory, Microporous Mesoporous Mater. 160 (2012) 47–66. doi:10.1016/j.micromeso.2012.04.043.

[90] A.S. Singha, A.K. Rana, Preparation and characterization of graft copolymerized Cannabis indica L. fiber-reinforced unsaturated polyester matrix-based biocomposites, J. Reinf. Plast. Compos. 31 (2012) 1538–1553. doi:10.1177/0731684412442989.

[91] Y. Jiang, M. Lawrence, M.P. Ansell, A. Hussain, Cell wall microstructure, pore size distribution and absolute density of hemp shiv, R. Soc. Open Sci. 5 (2018). doi:10.1098/rsos.171945.

[92] J.R. Dodson, Wheat straw ash and its use as a silica source, Univ. York. (2011) 302.

[93] N. Abd-Talib, A. Ahmad, S. Mohd-Setapar, A.K. Khamis, D. Lokhat, M. Rafatullah, Removal of silica from rice straw by using alkaline hydrogen peroxide solution in a fixed bed column, J. Mater. Environ. Sci. 9 (2018) 864–872. doi:10.26872/jmes.2018.9.3.95.

[94] pi.1355.pdf, (n.d.).

[95] I. Khouni, G. Louhichi, A. Ghrabi, P. Moulin, Efficiency of a coagulation/flocculation–membrane filtration hybrid process for the treatment of vegetable oil refinery wastewater for safe reuse and recovery, Process Saf. Environ. Prot. 135 (2020) 323–341. doi:10.1016/j.psep.2020.01.004.

[96] C. Shin, G.G. Chase, Water-in-Oil Coalescence in Micro-Nanofiber Composite Filters, AIChE J. 50 (2004) 343–350. doi:10.1002/aic.10031.

[97] J. Ge, J. Zhang, F. Wang, Z. Li, J. Yu, B. Ding, Superhydrophilic and underwater superoleophobic nanofibrous membrane with hierarchical structured skifile:///Users/Subbi/Documents/My Research/Theses/Manuscript 2/Literature Review/MF/anie.201308183 (1).pdfn for effective oil-in-water emulsion separation, J. Mater. Chem. A. 5 (2017) 497–502. doi:10.1039/c6ta07652a.

[98] Y. Du, Y. Li, T. Wu, A superhydrophilic and underwater superoleophobic chitosan-TiO2 composite membrane for fast oil-in-water emulsion separation, RSC Adv. 7 (2017) 41838–41846. doi:10.1039/c7ra08266e.

[99] A.P. Lim, A.Z. Aris, Continuous fixed-bed column study and adsorption modeling: Removal of cadmium (II) and lead (II) ions in aqueous solution by dead calcareous skeletons, Biochem. Eng. J. 87 (2014) 50–61. doi:10.1016/j.bej.2014.03.019.

[100] O. Abdelwahab, N.K. Amin, E.S.Z. El-Ashtoukhy, Electrochemical removal of phenol from oil refinery wastewater, J. Hazard. Mater. 163 (2009) 711–716. doi:10.1016/j.jhazmat.2008.07.016.